

## CHAPTER I

### Quartz Crystal Applications

By W. P. MASON

#### 1.1. INTRODUCTION—PURPOSE OF SERIES

**T**HIS paper is the first one of a series of papers dealing with quartz crystals, their applications in oscillators, filters, and transducers, and the methods of producing them from the natural crystal. This series was prepared first to make available to the Western Electric Co. and other manufacturers of quartz crystals some of the specialized knowledge on these subjects that has been acquired at the Bell Telephone Laboratories. Sufficient interest has been expressed in this series to make it desirable to publish them in serial form.

This first paper in the series is a general introductory paper covering the application of crystals to oscillators, filters and transducers. An appendix is given which discusses the elastic and electric relations in crystals and gives recent measurements of the elastic constants, their temperature coefficients, and the piezoelectric constants of quartz. This paper is followed by more detailed papers by Messrs. Bond, Willard, Sykes, McSkimin, and Fair which give consideration to quartz crystallography; determination of orientation by optical methods, X-ray methods, and etching methods; the imperfections occurring in quartz crystals; modes of motion and their calculation; the dimensioning of crystals to avoid undesirable resonances; and the use of crystals in oscillators.

#### 1.2 EARLY HISTORY OF PIEZOELECTRICITY AND ITS APPLICATIONS

The direct piezoelectric effect was discovered by the brothers Curie in 1880. They measured the effect first for a quartz crystal by putting a weight on the surface and measuring the charge appearing on the surface, the magnitude of which was proportional to the applied weight. A simple model for demonstrating this effect can be made by using a large piece of Rochelle salt cut with its length  $45^\circ$  from the  $Y$  and  $Z$  crystallographic axes and placing tinfoil electrodes normal to the  $X$  axis. If these electrodes are connected to a neon lamp, and the crystal is compressed by hitting it with a hammer, a charge is generated on the surface and a voltage applied to the lamp sufficient to break it down. In fact as much as 2000 volts can be generated by striking the crystal hard.

The converse piezoelectric effect was predicted in 1881 by the French physicist Lippmann on the basis of the principle of conservation of electricity. It was verified in the same year by the brothers Curie. In this effect a crystal is strained when a voltage is applied to it. The effect can be demonstrated by a model which consists of two thin pieces of Rochelle salt poled so that one expands when the voltage is applied and the other contracts. The result is—as in a bimetallic thermostat—the crystal bends. For crystals 10 mil inches thick and 4 inches long, a ninety-volt battery applied causes a displacement of a quarter of an inch or more of the end of the unit. Reversing the voltage reverses the direction of the displacement. The Curies constructed a bimorph unit of this type out of quartz and used it practically to measure voltage by measuring the displacement of the end of the crystal. By connecting the leads of an electrometer to the terminals, they could measure force applied by measuring the amount of charge generated at the terminals.

Outside of this use which was quite minor, the piezoelectric effect remained a scientific curiosity until the war of 1914–1918. It did inspire, however, considerable scientific speculation. Lord Kelvin in 1893 proposed a model for explaining the piezoelectricity of quartz and was able to calculate approximately the value of the piezoelectric constant. This model is discussed briefly in the next section. He also constructed and demonstrated a “piezoelectric pile” made from small spheres of zinc and copper, to illustrate the effect. At about the same time (1890–1892) Voigt published a series of papers followed by a book “Lehrbuch der Kristall Physik” (1910) in which the stresses, strains, fields and polarizations of piezoelectric crystals are related in mathematical form. These mathematical expressions (which are discussed further in the appendix) form a basis for the development of the properties of oriented crystals as discussed in section 1.5.

During the war of 1914–1918, Professor Langevin in Paris was requested by the French Government to devise some way of detecting submarines by acoustic waves they produce in water. After trying several devices he finally found that piezoelectric quartz plates could be used for that purpose. His device, which is shown in Fig. 1.1, consisted essentially of a mosaic of quartz which has the property that when a voltage is applied the crystal will expand and send out a longitudinal wave. Similarly, if a wave strikes it, the wave will set the quartz in vibration and generate a voltage which can be detected by vacuum tube devices. Langevin did not get his device perfected till after the war so it was not used at that time to detect submarines. Similar devices have, however, been used in this war. Langevin's original apparatus was used extensively as a sonic depth finder. In this use a pulse is generated which is recorded directly on a moving record and

is also sent out into the ocean. It strikes the bottom and is reflected back causing another mark to appear on the record. Knowing the difference in time and the velocity of sound in sea water, the distance to the bottom can be measured. A typical record is shown in Fig. 1.2. The top record shows the contour of the sea bottom while the second record shows the reflections from a school of fish.

At about the same time, Nicolson at Bell Telephone Laboratories was experimenting with Rochelle salt, another piezoelectric material having a

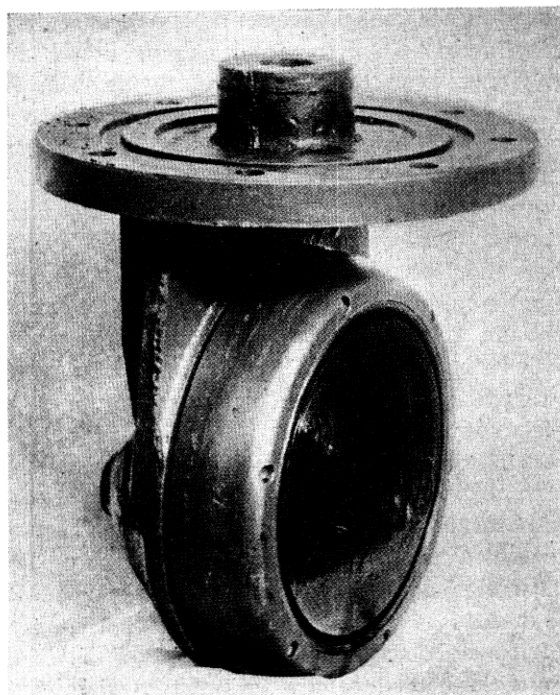


Fig. 1.1—Ultrasonic transmitting apparatus

much larger piezoelectric effect than quartz. He constructed and demonstrated loud speakers, microphones, and phonograph pick-ups using Rochelle salt.<sup>1</sup> He was also the first one to control an oscillator by means of a crystal—in this case Rochelle salt—and has the primary crystal oscillator patent.<sup>2</sup> Nicolson's circuit is shown in Fig. 1.3. The crystal is effectively in a path between the resonating coil in the output and the grid, since the electrode

<sup>1</sup> "The Piezoelectric Effect in the Composite Rochelle Salt Crystal"—A. M. Nicolson, *Proc. A. I. E. E.* 1919, 38, 1315.

<sup>2</sup> See Patent 2,212,845 filed April 10, 1918; issued Aug. 27, 1940.

3 is in the direction of the smallest piezoelectric effect in Rochelle salt and contributes little to the action. If terminal one to the tapped coil is at the top of the coil, the circuit although employing a three electrode crystal connection, effectively reduces to *B* in which the crystal is in the feedback path from plate to grid. On the other hand, if the tap is effectively at the bottom of the coil, the crystal is between grid and ground and feedback occurs through a distributed capacity from plate to grid. Both of these

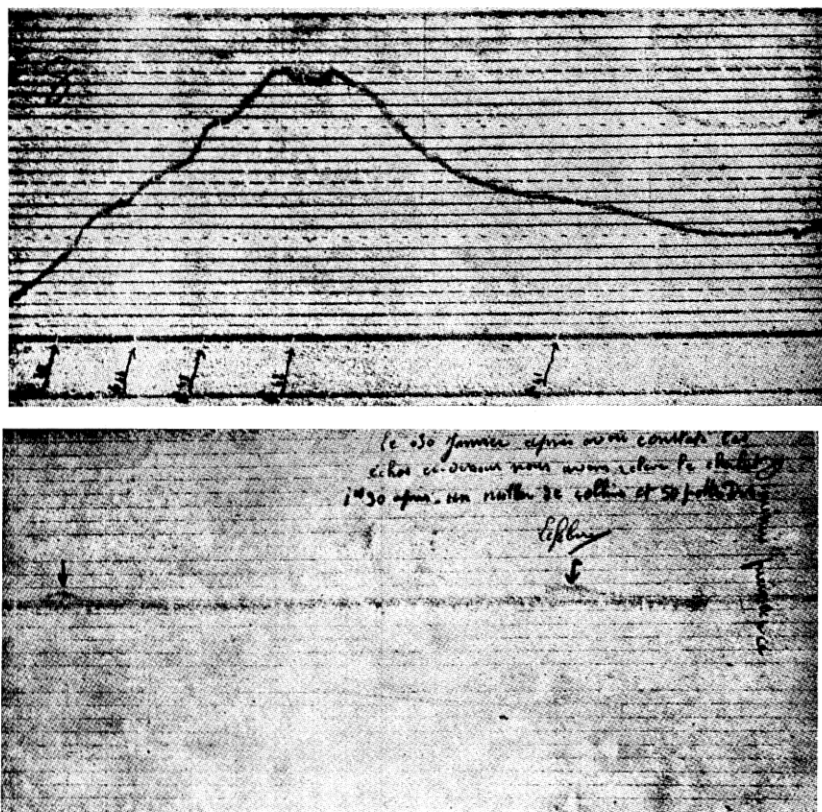


Fig. 1.2—Ocean contour curves

circuits *B* and *C* are widely used in oscillators of Pierce. Prof. G. W. Pierce published a circuit similar to circuit *B*, having a two electrode quartz crystal connected between grid and plate.<sup>3</sup>

In 1921, Professor Cady at Wesleyan University first showed<sup>4</sup> that quartz

<sup>3</sup> "Piezoelectric Crystal Resonators and Crystal Oscillators Applied to the Precision Calibration of Wave Meters," G. W. Pierce, Amer. Acad. of Arts and Sciences, Oct. 1923, 81-106.

<sup>4</sup> "The Piezoelectric Resonator" W. G. Cady, *Proc. I. R. E.* 1922, 10 83.

crystals could be used to control oscillators and that much more stable oscillators could be obtained in this fashion. These were later applied to controlling the frequency of broadcasting stations and radio transmitters in general and about 1925 Mr. W. A. Marrison applied them to obtain a very constant frequency and time standard, which is now used considerably by the Bell System, by radio broadcasting systems, and by power companies. The oscillators were subsequently improved by using crystals with small temperature coefficients as described in Section V. At the present time

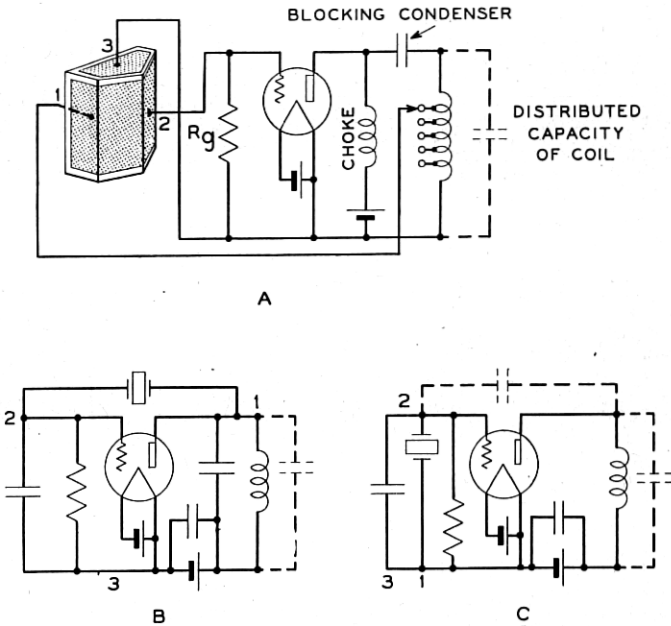


Fig. 1.3—Nicolson's oscillator circuit

crystal controlled oscillators are used very widely in radio military and commercial applications.

Another large use for quartz crystals is their use in providing very selective filters. Probably the first use of a crystal to select a narrow frequency range was made by Cady.<sup>4</sup> Using the very sharp maximum in current through a crystal at its resonant frequency, Cady proposed the use of such a crystal as a wave standard. This is equivalent to the use of a crystal as a tuned circuit. By incorporating a crystal in a three-winding transformer and balancing out the static capacity of the crystal by an auxiliary condenser, W. A. Marrison<sup>5</sup> improved the selecting ability of a crystal used

<sup>5</sup> Patent 1,994,658, filed June 7, 1927; issued March 19, 1935.

as a narrow band filter. At about the same time, L. Espenschied,<sup>6</sup> taking advantage of the knowledge of the equivalent electrical circuit of a crystal given previously by Van Dyke,<sup>7</sup> showed how to combine other electrical elements with crystals in ladder form to obtain band-pass filters. It was not, however, until the crystals were combined with auxiliary coils and condensers into the form of resistance compensated lattice type networks<sup>8</sup> that much progress was made in achieving the wide pass-band characteristics necessary for telephone and radio communication. Such filters have provided very selective devices which are able to separate one band of speech frequencies from another band different by only a small frequency percentage from the desired band. This property makes it possible to space channels close together with only a small frequency separation up to a high frequency, and such filters have had a wide use in the high-frequency carrier systems, and in the coaxial system which transmits more than 480 conversions over one pair of conductors. In radio systems such filters have been used extensively in separating one side band from the other in single side-band systems.

In conclusion we can say, that the science of piezoelectricity was born about 62 years ago, lay dormant for nearly 40 years, but during the last 25 years has advanced at such a rate that it can be regarded as one of the foundation stones of the whole communication art.

### 1.3. THEORY OF PIEZOELECTRIC MATERIALS

Piezoelectric crystals are of interest in communication circuits because they possess three properties. These properties are: (1) the piezoelectric effect provides a coupling between the electrical circuit and the mechanical properties of the crystal; (2) the internal dissipation of most crystals and particularly quartz crystals is very low, and the density and elastic constants of the crystals are very uniform, so that a crystal cut at a given orientation always has the same frequency constant; and (3), at specified orientations crystals can be cut which have advantageous mechanical properties such as a small change in frequency with a change in temperature, or a freedom from secondary modes of motion. It is the purpose of this section to discuss the first property, the coupling between the electrical and mechanical properties of the crystal.

The piezoelectricity of quartz and other materials is due to the fact that

<sup>6</sup> Patent 1,795,204, filed Jan. 3, 1927, issued August 8, 1933.

<sup>7</sup> K. S. Van Dyke; Abstract 52, *Phys. Rev.* June 1925; *Proc. I. R. E.* June 1928.

<sup>8</sup> See "Electrical Wave Filters Employing Quartz Crystals as Elements," W. P. Mason, *B. S. T. J.*, Vol. XIII, p. 405, July 1934; "Resistance Compensated Band Pass Crystal Filters for Unbalanced Circuits," *B. S. T. J.*, Vol. XVI, p. 423, Oct. 1937; "The Evolution of the Crystal Wave Filter," O. E. Buckley, *Jour. App. Phys.*, Oct. 1936; and Patents 1,921,035; 1,967,249; 1,967,250; 1,969,571; 1,974,081; 2,045,991; 2,094,044.

a pressure which deforms the crystal lattice causes a separation of the centers of gravity of the positive and negative charges thus generating a dipole moment (product of the value of the charges by their separation) in each molecule. How this separation can cause a coupling to an electrical circuit is illustrated by Fig. 1.4 which shows a crystal with metal electrodes normal to the direction of charge separation. If we short-circuit these electrodes and apply a stress which causes the centers of gravity of the charges to separate, free negative charges in the wire will be drawn toward the electrode in the direction of positive charge separation, and free positive charges in the wire will be drawn to the electrode in the direction of negative charge displacement until the crystal appears to be electrically neutral by any test conducted outside the crystal. When the stress is released the charges in the wire will flow back to their normal position. If, during the process, we connect an oscillograph in the short-circuited wire, there will be a pulse of current in one direction when the stress is applied and a pulse in the oppo-

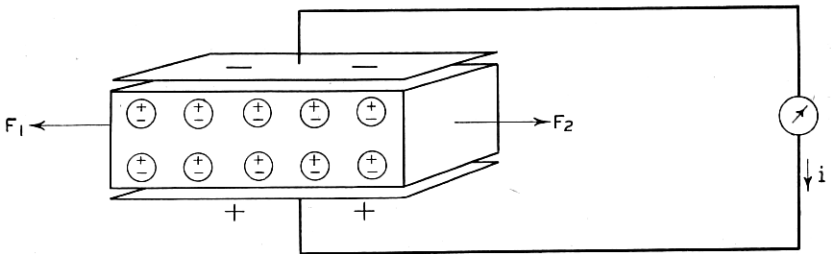


Fig. 1.4—Method for transforming mechanical energy into electrical energy in a crystal

site direction when the stress is released. By putting a resistance in the connecting wire and applying a sinusoidal stress to the crystal, an alternating current will flow through the load and consequently mechanical power will be changed into electrical power. Using the converse effect, a source of alternating voltage in the electrical circuit will produce an alternating stress in the crystal, and if this is working against a mechanical load, the electrical energy will be changed into mechanical energy.

To apply this concept to quartz let us consider Fig. 1.5, which represents the approximate arrangement of molecules in a quartz molecule. Lord Kelvin's explanation of the piezoelectricity of quartz is the following:

"The diagram (Fig. 1.5A) shows a crystalline molecule surrounded by six nearest neighbors in a plane perpendicular to the optic axis of a quartz crystal. Each silicon atom is represented by + (plus) and each oxygen double atom - (minus). The constituents of each cluster must be supposed to be held together in stable equilibrium in virtue of their chemical affinities. The different clusters, or crystalline molecules, must be supposed to be relatively mobile before taking

positions in the formation of a crystal. But we must suppose, or we may suppose, the mutual forces of attraction (or chemical affinity), between the silicon of one crystalline molecule and the oxygen of a neighboring crystalline molecule, to be influential in determining the orientation of each crystalline molecule, and in causing disturbance in the relative positions of the atoms of each molecule, when the crystal is strained by force applied from without.

“Imagine now each double atom of oxygen to be a small negatively electrified particle, and each atom of silicon to be a particle electrified with an equal quantity of positive electricity. Suppose now such pressures, positive and negative, to be applied to the surface of a portion of crystal as shall produce a simple elongation in the direction perpendicular to one of the three sets of rows. This strain is indicated by the arrow heads in Fig. 1.5A and is realized to an exaggerated extent in Fig. 1.5B.

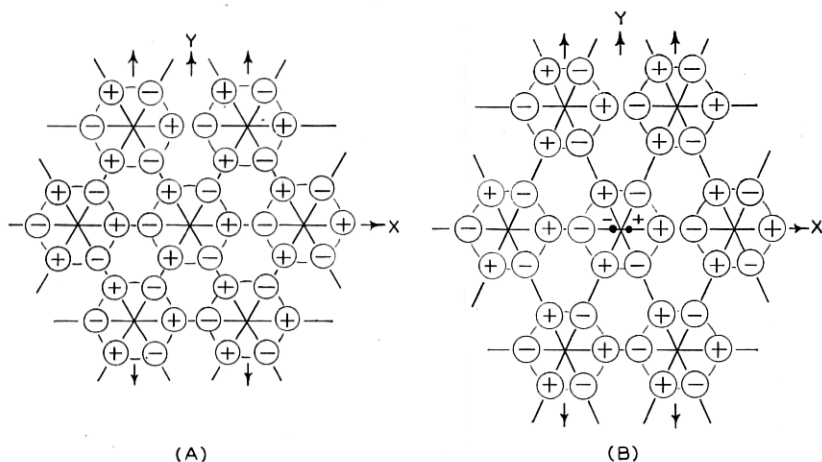


Fig. 1.5—Kelvin's model of quartz molecules

“This second diagram shows all the atoms and the centers of all the crystalline molecules in the positions to which they are brought by the strain. Both diagrams are drawn on the supposition that the stiffness of the relative configuration of atoms of each molecule is slight enough to allow the mutual attractions between the positive atoms and the negative atoms of neighboring molecules to keep them in line through the centers of the molecules, as Fig. 1.5A shows for the undisturbed condition of the systems, and Fig. 1.5B for the system subjected to the supposed elongation. Hence two of the three diameters through atoms of each crystalline molecule are altered in direction, by the elongation, while the diameter through the third pair of atoms remains unchanged, as is clearly shown by Fig. 1.5B compared to Fig. 1.5A.

“Remark, first that the rows of atoms, in lines through the centers of the crystalline molecules, perpendicular to the direction of the strain, are shifted to parallel positions with distances between the atoms in them unchanged. Hence the atoms in these rows contributed nothing to the electrical effect. But in parallel to these rows, on each side of the center of each molecule, we find two pairs of atoms whose distances are diminished.



"This produces an electrical effect which, for great distances from the molecule, is calculated by the same formula as the magnetic effect of an infinitesimal bar magnet whose magnetic moment is numerically equal to the product of the quantity of electricity of a single atom into the sum of the diminutions of the two distances between the atoms of the two pairs under consideration. Hence, denoting by  $N$  the number of crystalline molecules per unit bulk of the crystal; by  $b$  the radius of the circle of each crystalline molecule; by  $q$  the quantity of electricity of each of the six atoms or double atoms, whether positive or negative; by  $\theta$  the change of direction of each of the two diameters through atoms which experience change of direction; and by  $\mu$  the electric moment developed per unit volume of the crystal, by the strain which we have been considering and which is shown in Fig. 1.5B; we have

$$\mu = N q 4 b \theta \cos 30^\circ = 2\sqrt{3} N b q \theta \quad (1.1)''$$

Kelvin's model shows some of the symmetry properties of quartz. The axis marked  $X$  is the  $X$  or electrical axis of the crystal. The  $Z$  or optic axis is normal to the plane of the paper. The  $Y$  or mechanical axis is the axis

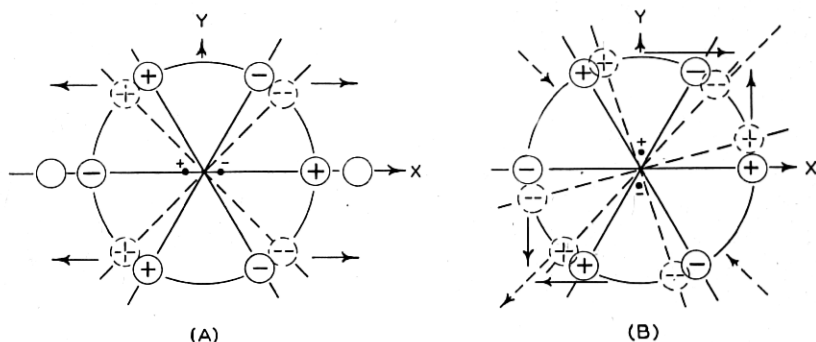


Fig. 1.6—Longitudinal and shear strains applied to a quartz molecule

along which the stress is applied. It is obvious that if we rotate the direction of the applied stress by  $120^\circ$ , a similar separation of charges at right angles to the stress will occur. There are then three electrical axes and three mechanical axes so that the optic axis can be regarded as an axis of threefold symmetry for the crystal.

As can be shown from an extension of Kelvin's model there are two other types of stresses that will produce a charge separation normal to the axis. Suppose that we stress the crystal along the  $X$  or electrical axis as shown by Fig. 1.6A. Applying the same reasoning as before, we see that the apex molecules are separated farther apart without changing the separation between the other molecules. This results in a separation of the centers of gravity of the positive and negative charges, with the negative charges moving toward the left and the positive charges moving toward the right. The separation is still along the electric axis, but is in the opposite direction

to that caused by a stress along the  $Y$  axes. A detailed analysis shows that the value of the electrical separation moment (dipole moment) for a stress along either axis is the same value but the sign is reversed. A longitudinal stress then can only produce a charge moment along the  $X$  or electrical axis which is the origin of the name electrical axis.

If, however, we introduce a different kind of stress known as a shearing stress, a separation of centers of charges can occur along the mechanical or  $Y$  axis of the crystal. A simple shear stress is one in which forces act normal to the direction of space separation rather than along it as shown, for example, by the two opposed arrows normal to the mechanical axis in Fig. 1.6B. Such a shear does not occur in nature, but rather a pure shear which consists of two simple shears which are directed in such a way as to produce no rotation of the molecule as a whole about its axis. If we resolve these force components along directions  $45^\circ$  from the crystal axes, a pure shear is equivalent to an extensional stress along one  $45^\circ$  axis and a compressional stress along the other  $45^\circ$  axis. Such a stress would cause the charges to be displaced from their normal position, as shown in the figure. This causes the center of positive charge to be displaced downward along the mechanical or  $Y$  axis of the crystal while the center of negative charge is displaced upward along the mechanical axis.

These three relations can be written in the form

$$P_x = -d_{11}X_x + d_{11}Y_y ; \quad P_y = 2d_{11}X_y \quad (1.2)$$

where  $P_x$  is the polarization or charge per unit area developed on an electrode surface normal to the  $X$  axis due to the applied longitudinal stresses  $X_x$  and  $Y_y$ , while  $P_y$  is the polarization normal to the  $Y$  axis caused by the shearing stress  $X_y$ .  $d_{11}$  is the piezoelectric constant and equations (1.2) show that the magnitudes of all these effects are closely related. In addition to these three major piezoelectric effects, quartz has two smaller effects which, since they are connected with the distribution of molecules in the  $YZ$  and  $XZ$  planes, cannot be demonstrated by the figures given previously. The complete piezoelectric relations are then

$$P_x = -d_{11}X_x + d_{11}Y_y - d_{14}Z_z ; \quad P_y = d_{14}Z_z + 2d_{11}X_y \quad (1.3)$$

where  $Y_z$  and  $Z_x$  are respectively similar shearing stresses exerted in the  $YZ$  and  $ZX$  planes respectively. The best values for the  $d_{11}$  and  $d_{14}$  constants are respectively

$$d_{11} = -6.76 \times 10^{-8} \frac{\text{e.s.u.}}{\text{dyne}} ; \quad d_{14} = 2.56 \times 10^{-8} \frac{\text{e.s.u.}}{\text{dyne}} \quad (1.4)$$

as obtained by recent measurements for a number of  $X$  cut and rotated  $X$ -cut crystals discussed in appendix A.

Quartz is not the only type of crystal which is piezoelectric. In fact there are hundreds of crystals that exhibit this property. Whether a crystal is piezoelectric or not and the relation between the stresses and charge displacements depend on the symmetry of the crystal. Whenever there is a center of symmetry; that is, when the properties of the crystal are the same in both directions along any line, no piezoelectric effect can occur. This is illustrated by the simple arrangement of atoms shown by Fig. 1.7. It is obvious that no symmetrical application of forces can separate the center of gravity of the charges and hence such a crystal will not be

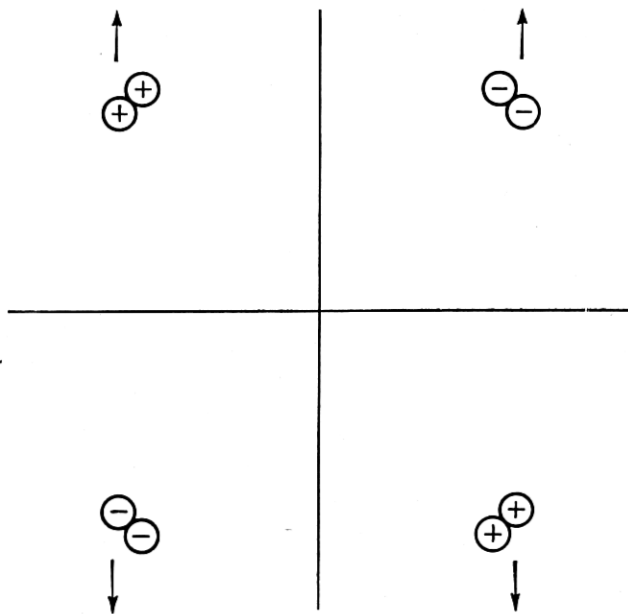


Fig. 1.7—Crystal with a center of symmetry

piezoelectric. Crystals can be classified into 32 possible classes on the basis of the symmetry they exhibit; and of these 32 classes, 20 are piezoelectric and 12 are not. As illustrated by the model for quartz, the response to different types of force depends solely on the type of symmetry existing in the crystal.

#### 1.4. ELECTRICAL IMPEDANCE AND LOW DISSIPATION IN CRYSTALS

The first crystal used by Cady in controlling oscillators, was a crystal cut with its major faces perpendicular to the  $X$  or electrical axis and with its length along the  $Y$  or mechanical axis. Referring to Fig. 1.5B, we see that a stretch along the  $Y$  axis will produce a charge displacement along the  $E$

or  $X$  axis. Conversely, a voltage applied along the  $X$  axis will produce a charge displacement and consequently a mechanical stress along the  $Y$  axis which will set up a longitudinal wave along the mechanical axis. As shown by Fig. 1.8, the type of motion resulting when the crystal is free to move on the ends is one in which the center is stationary and the ends move in and out. The crystal can then be clamped at its center or mounted from leads soldered to electrodes deposited on the surface.

In using a crystal in an electrical circuit it is desirable to have an electrical equivalent circuit which will represent the electrical impedance as measured from the terminals of the crystal. Such a circuit<sup>9</sup> is shown in Fig. 1.8. In

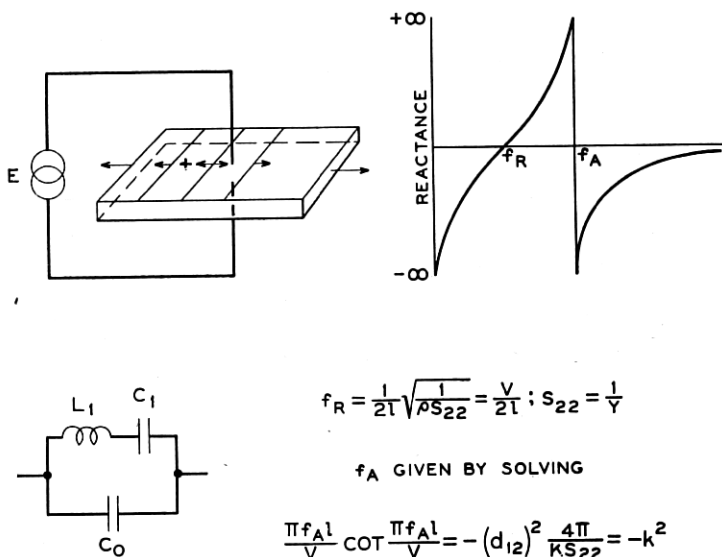


Fig. 1.8—Longitudinally vibrating crystal and electrical equivalent circuit

this representation  $C_0$  is the static capacity of the crystal which would be measured if the crystal were held from moving.  $C_1$  is the stiffness of the crystal transformed into electrical terms through the piezoelectric effect of the crystal, while  $L_1$  is the effective mass of the crystal also transformed into electrical terms. The resonant frequency of the crystal is determined by the Young's modulus and density of the bar according to the usual formula:

$$f_R = \frac{1}{2l} \sqrt{\frac{Y_0}{\rho}} \tag{1.5}$$

<sup>9</sup> Circuits of this type for representing the electrical impedance of a crystal were first derived by Van Dyke; see reference (7). The method of deriving them from Voigt's equations is discussed in the appendix.

where  $Y_0$  is the value of Young's modulus along the bar,  $\rho$  the density, and  $l$  the length of the bar.

A significant feature of the equivalent circuit is that there is always a definite ratio between  $C_0$  and  $C_1$  for a given crystal cut. This is really a measure of the ratio of electrical to mechanical energy stored in the crystal under an applied constant voltage. The reactance characteristic of the network is shown by Fig. 1.8 as a function of frequency. The reactance starts out as a negative reactance at low frequencies, becomes zero at the resonant frequency  $f_R$ , becomes positive and very large at the anti-resonant frequency  $f_A$ , then again becomes a negative reactance. Due to the high ratio of  $C_0$  to  $C_1$  existing in a crystal the separation between  $f_A$  and  $f_R$  becomes very small. For example, for an  $AT$  crystal this ratio is around 200 and the separation of  $f_A$  from  $f_R$  is only a quarter of a per cent in frequency. Since it can be shown that an oscillator will only oscillate on the positive reactance part of the crystal characteristic, the narrow separation between resonant and anti-resonant frequencies explains why a crystal can act as such a good stabilizer for an oscillator. As long as the crystal resonance itself does not change with temperature or other conditions, the very sharp reactance frequency characteristic will not allow the oscillator frequency to change much with a change in oscillator voltage, tube conditions, or any other changes which are likely to cause a change in frequency for a coil and condenser controlled oscillator.

Strictly speaking, a resistance should be added in series with the inductance  $L_1$  to represent the internal losses in the crystal, the loss of energy at the clamping points and the loss of energy due to setting up of air waves by the crystal motion. However, the value of this resistance and the amount of energy lost is very small in a crystal compared to what the losses are in purely electrical elements. A demonstration which shows this effect and shows that most of the losses of a well mounted longitudinally vibrating crystal are acoustic losses caused by setting up air waves in the vicinity of the crystal, can be made by using two oscillators, one a fixed oscillator and the other one controlled by a resonant circuit or a crystal. The fixed oscillator may be set at 99 kilocycles and the crystal oscillator controlled by a 100-kc crystal. The two will beat together giving the 1000-cycle note. When the battery is taken off the crystal oscillator, it continues to oscillate till the energy built up in the crystal is dissipated in the internal dissipation of the crystal. A good electrical circuit which has a ratio of reactance to resistance, or  $Q$  of the coil of 300 dies down almost instantaneously. For a crystal mounted in air it takes about half a second to become inaudible. This corresponds to a  $Q$  of 30,000 where  $Q$  is defined as the ratio of the reactance of the coil  $L_1$  of Fig. 1.8 to the resistance. For a crystal mounted in a vacuum a much higher  $Q$  is obtained due to the elimination of the loss of energy by acoustic radiation. For such a crystal it takes eight

seconds to die down which corresponds to a  $Q$  of 330,000, which is about 1000 times as great as that for a good electrical circuit.

### 1.5. MODES OF MOTION AND CRYSTAL ORIENTATION TO PRODUCE LOW TEMPERATURE COEFFICIENT CRYSTALS

As mentioned previously the first crystal cut used in oscillators was a longitudinal vibration along the  $Y$  or mechanical axis excited by a field applied

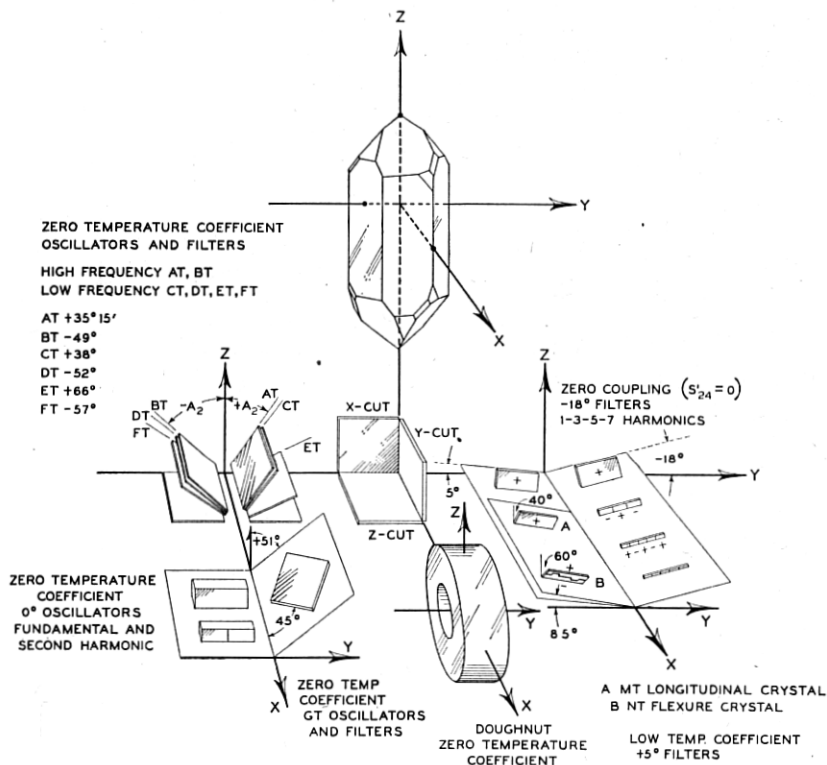


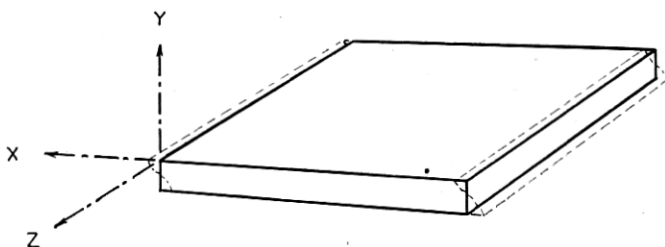
Fig. 1.9—Oriented quartz crystal cuts in relation to the natural crystal

along the electrical or  $X$  axis. This mode gives a good resonance free from other modes and a modification of it is now used in crystal filters. This modification, as shown by Fig. 1.9, ( $-18.5^\circ$  filter crystal) consists in rotating the direction of the length by  $18.5^\circ$  from the  $Y$  or mechanical axis, about the  $X$  or electrical axis. As described previously<sup>10</sup>, the effect of this rotation is to eliminate the coupling between the desired longitudinal mode and the undesired face shear mode, thus simplifying the motion and eliminating an

<sup>10</sup> "Electrical Wave Filters Employing Quartz Crystals as Elements," W. P. Mason, *B. S. T. J.*, Vol. XIII, p. 405 July 1934 or patent 2,173,589.

undesired resonance. However, to get a reasonably high frequency out of a length vibrating type of cut requires too small a length to be practical.

It was not long before crystal oscillators were controlled by thickness vibrating crystals whose frequencies were determined by the thickness of the crystals or by their smallest dimension. Referring to Fig. 1.6A, we see that the same *X* cut type of crystal will generate a vibration along the electrical or *X* axis when a field is applied along this axis. Since the thickness dimension can be made very small, a high frequency is obtainable. However, when the smallest dimension is used to control the frequency, a difficulty arises not present when the largest dimension is used to control the frequency, namely, that harmonics and overtone modes of all the lower frequency types of motion produce frequencies near the frequency of the thickness mode and it is difficult to pick out the desired mode. This was



$$\delta X = A \cos \frac{n\pi Y}{a} \cos 2n\pi ft$$

$$f = \frac{n}{2t} \sqrt{\frac{c_{66}}{\rho}} ; \quad n=1, 3, 5 ; \quad c_{66} = \frac{c_{11} - c_{12}}{2}$$

Fig. 1.10—High frequency shear mode of motion

especially true for the thickness vibrating *X* cut crystal and led to its abandonment in favor of *Y* cut crystals vibrating in shear.

As seen from Fig. 1.6B, when a voltage is applied along the *Y* or mechanical axis, a shear vibration is produced which tends to change a square into a rhombus. For a large plate in which the edge dimensions are large compared to the thickness, the motion occurs as shown by Fig. 1.10. For such a plate the motion is perpendicular to the thickness, which is the direction of transmission of the wave, and hence a shear wave is sometimes called a transverse wave. The frequency of such a wave can be shown to be

$$f = \frac{1}{2t} \sqrt{\frac{c_{66}}{\rho}} \quad (1.6)$$

where *t* is the thickness of the plate,  $c_{66}$  is the shear stiffness constant and  $\rho$  the density. The use of *Y* cut plates considerably improved the per-

formance of oscillators since the plates do not have as many secondary modes of motion as do the  $X$  plates. They have, however, one drawback. The frequency increases about 86 parts in a million for every degree Centigrade increase in temperature. This requires regulating the temperature quite closely.

In order to improve on the performance of the  $Y$  cut crystal, investigations were made by Lack, Willard and Fair, Koga, Bechmann, Straubel and others<sup>11</sup> on how the properties of such crystals varied as the orientation angle of cutting blanks from the natural crystal was varied. As shown by Fig. 1.9, the crystals investigated all had one edge along the  $X$  or electrical axis with the normals making positive and negative angles with the  $Y$  axis. All of these crystals will have a component of field along the  $Y$  axis, which

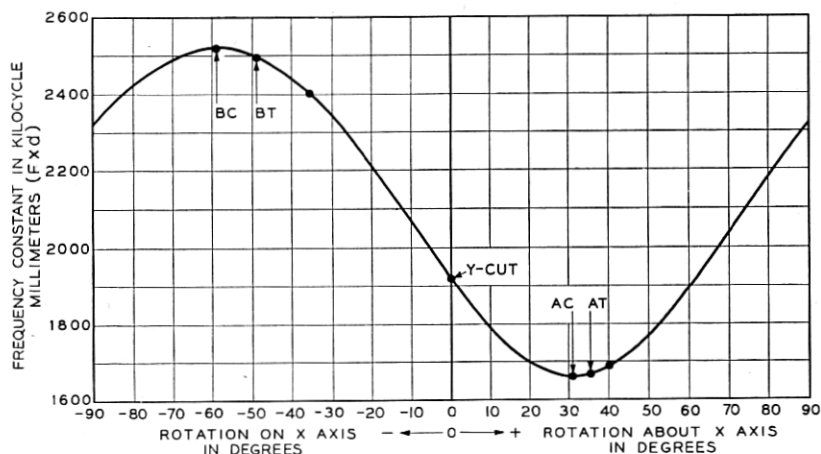


Fig. 1.11—Frequency constant of oriented  $Y$  cut crystals

will produce a shearing motion until the angles of cut approach 90 degrees from the  $Y$  axis. The smaller the angle  $A_2$  the more strongly will the shear mode be driven. However, advantageous elastic relationships can be obtained by using oriented cuts. As shown by Fig. 1.11, Lack, Willard and Fair found that the frequency constant of a rotated crystal expressed in kilocycle millimeters varied with angle of cut and that there was a minimum frequency at +31 degrees and a maximum at -59 degrees. It was subsequently pointed<sup>12</sup> out that these minimum and maximum points were significant angles in the elastic behavior of the crystal for they were the angles for

<sup>11</sup> "Some Improvements in Quartz Crystal Circuit Elements," F. R. Lack, G. W. Willard, I. E. Fair—*B. S. T. J.*, Vol. 13, pp. 453-463, July 1934; R. Bechmann—*HF Techn. u. El. Ak.* 44, 145 (1934); I. Koga—*Rep. of Rad. Res. i. Jap.* 6, 1 (1934); J. Straubel, *Z. tech. Physik.*, 35, 179, 1934.

<sup>12</sup> See patent 2,173,589.



which the high-frequency shear mode had zero coupling with the troublesome low-frequency shear mode system of vibrations. Crystals cut at these angles have a much cleaner frequency spectrum than *Y* cut crystals. Lack, Willard, and Fair also found that the temperature coefficient of frequency varied with angle as shown by Fig. 1.12. Starting from a high positive value for the *Y* cut, the coefficient becomes zero at an angle of  $+35^\circ - 15'$  and  $-49^\circ$ . The first angle cut is known as the *AT* cut and the second as the *BT* cut. Since the *AT* angle is nearer the *Y* cut, the piezo-electric constant is larger and it is more strongly driven than the *BT*. On the other

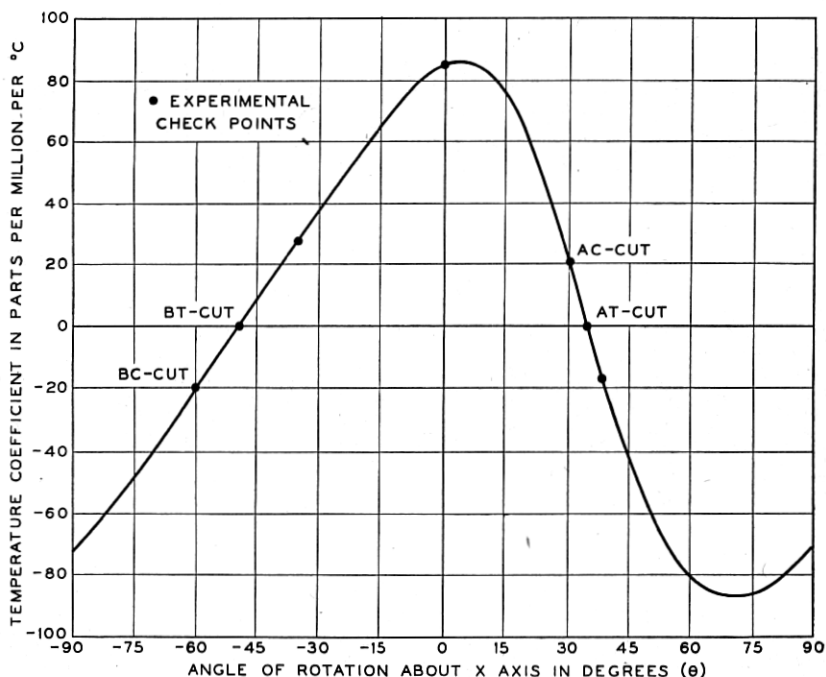


Fig. 1.12—Temperature coefficients of oriented *Y* cut crystals

hand, the *BT* has a higher frequency for the same thickness. Both crystals are near enough to the *AC* and *BC* cuts so that the systems of low-frequency shear modes are rather weakly driven. On the other hand, the shear mode of both crystals is rather strongly coupled to flexure modes of motion, as will be discussed by Mr. Sykes in a later chapter, and the crystal has to be exactly dimensioned in order that the flexure frequencies and other disturbing frequencies will not coincide with the desired shear mode.

Other oriented shear crystals for lower frequency work are the *CT* and *DT* crystals investigated by Willard and Hight. They are related to the *AT* and *BT* crystals as shown by Fig. 1.13. The plate on the right shows the

motion of an *AT* plate. If we were to increase the thickness dimension until the plate was nearly square, the *AT* motion would correspond to a face shear mode which should be controlled by the same elastic constants as the *AT* motion. At the same time in order to drive the crystal efficiently we could decrease the width until it became the thickness. This procedure would be the same as cutting a crystal at right angles to the *AT* and would suggest that by so doing we should obtain a low-frequency shear crystal with a low coefficient. Actually, Willard and Hight found that a crystal

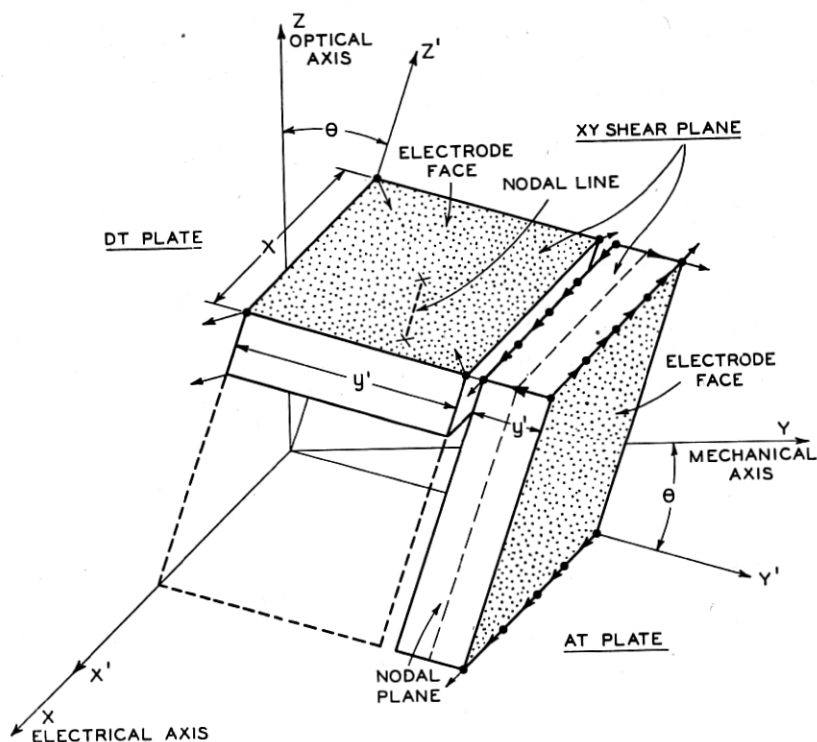


Fig. 1.13—Relation of *AT* and *DT* low temperature coefficient crystals

at  $-52^\circ$  or  $87^\circ$  from the *AT* would give a low coefficient. This crystal was called the *DT*. Similarly, a crystal cut at  $+38^\circ$  or  $87^\circ$  from the *BT* would also give a low coefficient and this has been called the *CT*. It can be shown that a component of the voltage applied along the mechanical axis will drive the shearing type of motion. The *CT* is larger for the same frequency and more strongly driven than the *DT*. It is extensively used in controlling oscillators in the frequency range from 200 to 500 kilocycles.

Quite a few other crystal cuts have been discovered as shown by Fig. 1.9.

Another important cut is the  $GT$ ,<sup>13</sup> which has a very constant frequency over a wide temperature range. As shown by Fig. 1.14, all zero temperature coefficient crystals are zero coefficient at one temperature only and usually vary in a square law curve about this temperature. The  $GT$  crystal represented an attempt to get a crystal in which the frequency remained constant over a wide temperature range. As can be seen from the figure, when properly adjusted this aim is attained, for the frequency does not vary more than one part in a million over a 100-degree Centigrade range of temperature.

This crystal makes use of the fact that a face shear vibration can be resolved into two longitudinal vibrations coupled together. As shown by

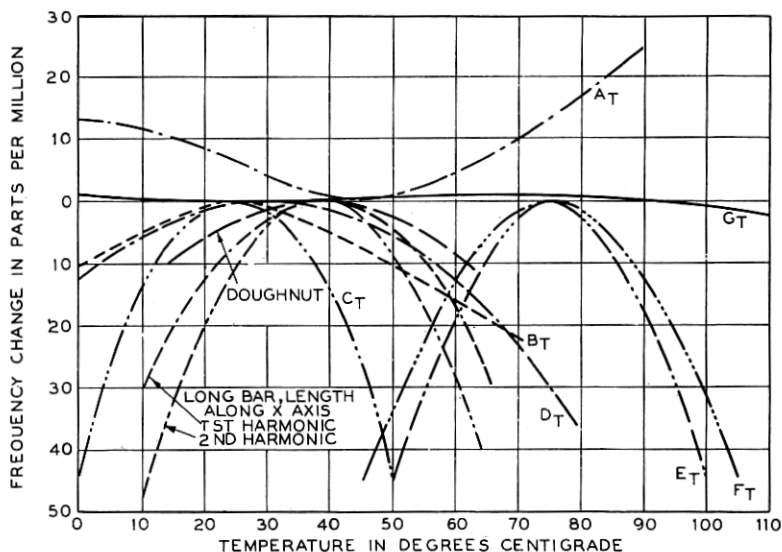


Fig. 1.14—Temperature frequency characteristics of a number of low temperature coefficient crystals

Fig. 1.15, if we cut a crystal at an angle of 45 degrees from that of a shear vibrating crystal, an expansion occurs along one axis and a contraction along the other indicating that a face shear can be resolved into two longitudinal modes that are coupled together. Now since it can be shown that all pure longitudinal modes for blanks cut in all possible directions in a quartz crystal will have zero or negative temperature coefficients,<sup>14</sup> it follows that if we have a shear vibrating crystal with a positive coefficient, that

<sup>13</sup> "A New Quartz Crystal Plate, Designated the  $GT$ , Which Produces a Very Constant Frequency Over A Wide Temperature Range," W. P. Mason, *Proc. I. R. E.*, Vol., 28 pr. 220-223, May 1940

<sup>14</sup> This can be proved as discussed in the appendix by combining the Voigt expressions for the elastic relations in a crystal with the measured temperature coefficients of the six elastic constants.

coefficient must have been caused by the coupling between the two modes. As a result of this observation it follows that if we have a shear vibrating crystal with a positive temperature coefficient and cut another crystal at 45 degrees from this crystal, the strong coupled mode which corresponds to the shear vibration will also have a positive temperature coefficient. As we grind down on the side, the two modes become farther apart in frequency and less closely coupled. Then, since they both will have a negative coefficient if separated far enough, it follows that for some ratio of axes, one of the modes will have a zero coefficient. This was tested out for a series of orientations near the *CT* and *DT* with the results shown in Fig. 1.16. Positive angle crystals had zero coefficients at ratios of axes varying from 1 to .855

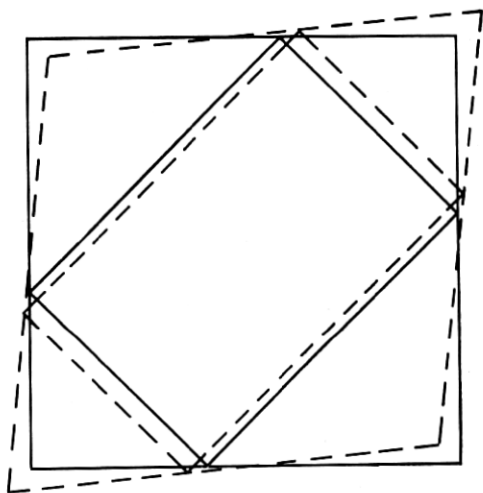


Fig. 1.15—Relation between a face shear mode and two coupled longitudinal modes

depending on the angle while negative angle crystals had zero coefficients at ratios from .64 to 1.0. For positive angle crystals it was the higher frequency mode that was the stronger and could be given the zero coefficient, while for the negative angle crystals it was the lower frequency mode that was the stronger and corresponded to the face shear mode.

Several of the positive angle crystals were measured over a temperature range with the results shown by Fig. 1.17. For angles above  $51^{\circ}-30'$  the curvature was positive, while for angles below  $51^{\circ}-30'$  the curvature was negative. Right at  $51^{\circ}-30'$  the large square law curvature term disappeared and the frequency was constant to one part in a million over a 100-degree Centigrade range centered at  $50^{\circ}\text{C}$ . as shown by Fig. 1.18. Some further experiments showed that this flat range could be moved around a bit by

changing the angle of cut and the ratio of axes simultaneously. To go from  $-25^{\circ}\text{C.}$  to  $+75^{\circ}\text{C.}$  with a mid-range at  $25^{\circ}\text{C.}$ , a crystal cut at  $51^{\circ}-7.5'$

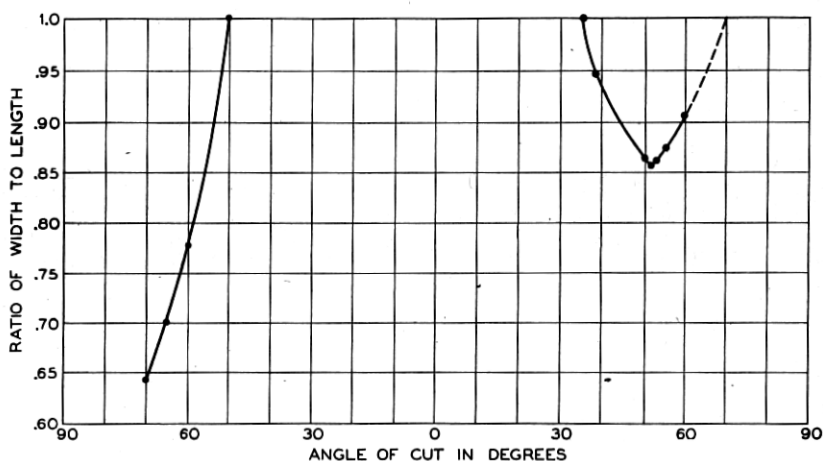


Fig. 1.16.—Relation between angle of cut and ratio of width to length for zero temperature coefficient for *G* type crystals

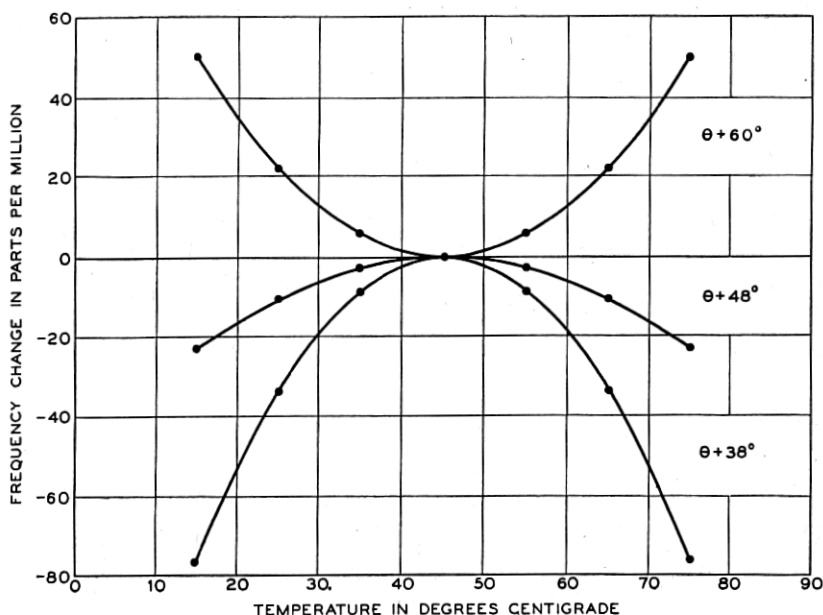


Fig. 1.17—Temperature frequency relations for various angles for *G* type crystals with a ratio of axes of 0.859 is required. The *GT* crystal has been used quite extensively in frequency and time standards and in filters meeting rigid phase requirements.

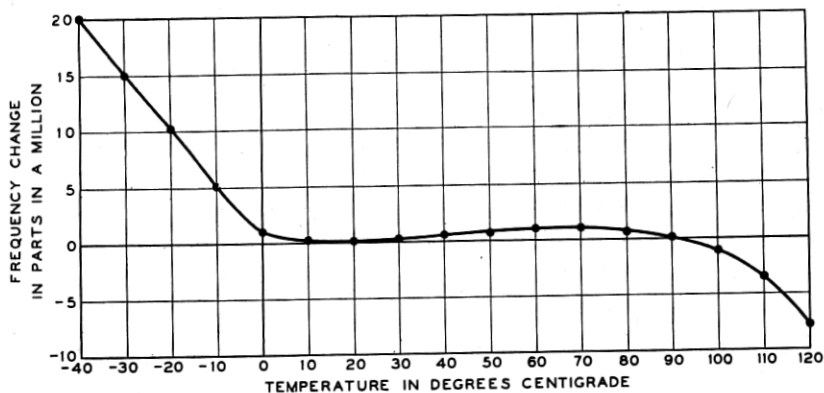


Fig. 1.18—Temperature frequency characteristic for GT crystal

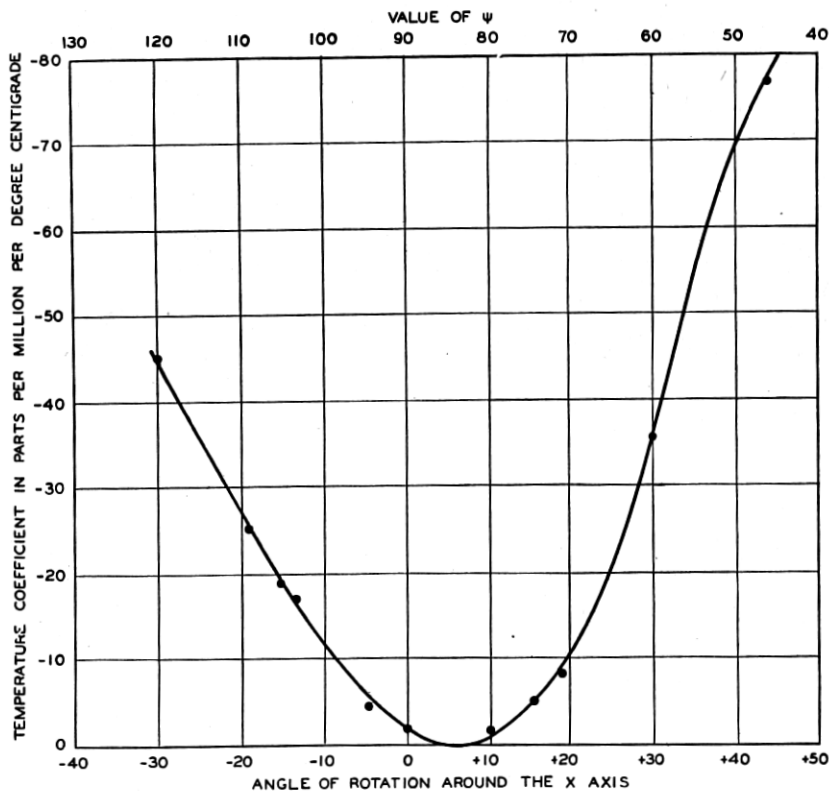


Fig. 1.19—Temperature coefficients of long thin rotated X cut crystals. Angle of rotation measured between length and Y axis. Dots are measured points. Solid line calculated from temperature coefficients evaluated in the appendix.

Two other cuts not previously described are shown also by Fig. 1.9. They are the *MT* low coefficient longitudinally vibrating crystal and the *NT* low coefficient flexurally vibrating crystal. Both of these are related to the  $+5^\circ X$  cut crystal of Fig. 1.9. As shown by Fig. 1.19 a long thin  $5^\circ X$  cut crystal is the best length direction for an *X* cut crystal to obtain a low-temperature coefficient. Figure 1.19 plots the temperature coefficients for long thin oriented *X* cut crystals, and this data is used in the appendix to derive the temperature coefficients of the six elastic constants. However, as the width of the crystal is increased the temperature coefficient becomes highly negative as shown by Fig. 1.20.

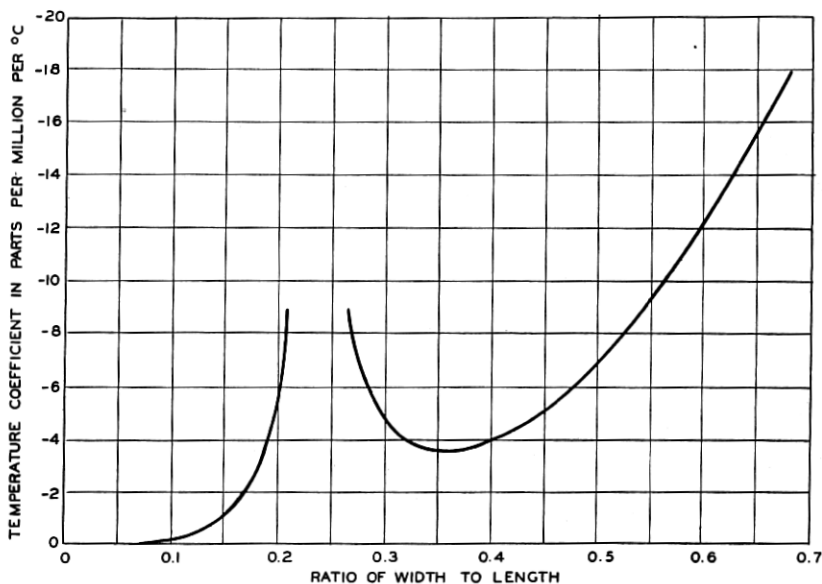


Fig. 1.20—Temperature coefficient of  $a +5^\circ X$  cut crystal ( $\varphi = 0^\circ; \theta = 90^\circ; \psi = 85^\circ$ ) as a function of the ratio of width to length. Ratio of thickness to length = 0.05.

This change of coefficient occurs due to the fact that as the crystal width is increased, the face shear mode of motion becomes more strongly excited and contributes to the elastic constant. Then since the temperature coefficient of the shear elastic constant is highly negative for this orientation the temperature coefficient of the  $+5^\circ X$  cut crystal becomes more highly negative as the width is increased.

The *MT* longitudinally vibrating crystal employs a rotation of the plane of the crystal cut about the  $Y'$  or length axis. The effect of this rotation is to change the temperature coefficient of the shear mode from highly negative to nearly zero. The result is that the temperature coefficient becomes

very low and nearly independent of the width length ratio. The *NT* low coefficient flexurally vibrating crystal is similar to the *MT* but requires a somewhat higher rotation about the  $Y'$  axis to produce a low coefficient.

The *MT* crystal has been used in narrow band filters such as pilot channel filters of the cable carrier system and in oscillators having frequencies between 50 kilocycles and 100 kilocycles. The *NT* flexure crystal is capable of producing frequencies as low as 4 kilocycles, and can be used to produce filters and control oscillators in the frequency range from 4 kilocycles to 50 kilocycles. Crystals of this type have been used with the Western Electric frequency modulation broadcast transmitter.<sup>15</sup> Operating in the region of 5 kilocycles, they maintain the frequency of the transmitter to  $\pm 0.0025$  per cent without temperature regulation. These two crystals will be described in more detail in a subsequent paper.

## APPENDIX A

### VOIGT'S ELASTIC AND PIEZOELECTRIC RELATIONS AND THEIR APPLICATION TO THE DETERMINATION OF LOW TEMPERATURE COEFFICIENT CRYSTALS

#### A.1 MATHEMATICAL EXPRESSIONS FOR PIEZOELECTRIC RELATIONS

As mentioned in the historical introduction, Voigt formulated a mathematical relation between the stresses, strains, polarizations, and electric fields existing in a crystal. For a general crystal devoid of symmetry these relations take the form

$$\begin{aligned}
 -x_x &= s_{11}^E X_x + s_{12}^E Y_y + s_{13}^E Z_z + s_{14}^E Y_z + s_{15}^E Z_x \\
 &\quad + s_{16}^E X_y - d_{11} E_x - d_{21} E_y - d_{31} E_z \\
 -y_y &= s_{21}^E X_x + s_{22}^E Y_y + s_{23}^E Z_z + s_{24}^E Y_z + s_{25}^E Z_x \\
 &\quad + s_{26}^E X_y - d_{12} E_x - d_{22} E_y - d_{32} E_z \\
 -z_z &= s_{31}^E X_x + s_{32}^E Y_y + s_{33}^E Z_z + s_{34}^E Y_z + s_{35}^E Z_x \\
 &\quad + s_{36}^E X_y - d_{13} E_x - d_{23} E_y - d_{33} E_z \\
 -y_z &= s_{41}^E X_x + s_{42}^E Y_y + s_{43}^E Z_z + s_{44}^E Y_z + s_{45}^E Z_x \\
 &\quad + s_{46}^E X_y - d_{14} E_x - d_{24} E_y - d_{34} E_z
 \end{aligned}
 \tag{A.1}$$

<sup>15</sup> "A New Broadcast Transmitter Circuit Design for Frequency Modulation," J. F. Morrison, *Proc. I. R. E.*, Vol. 28, No. 10, Oct. 1940, pp. 444-449.



$$\begin{aligned}
 -z_x &= s_{51}^E X_x + s_{52}^E Y_y + s_{53}^E Z_z + s_{54}^E Y_z + s_{55}^E Z_x \\
 &\quad + s_{56}^E X_y - d_{15} E_x - d_{25} E_y - d_{35} E_z \\
 -x_y &= s_{61}^E X_x + s_{62}^E Y_y + s_{63}^E Z_z + s_{64}^E Y_z + s_{65}^E Z_x \\
 &\quad + s_{66}^E X_y - d_{16} E_x - d_{26} E_y - d_{36} E_z \\
 P_x &= -d_{11} X_x - d_{12} Y_y - d_{13} Z_z - d_{14} Y_z - d_{15} Z_x - d_{16} X_y + \kappa_1^F E_x \\
 P_y &= -d_{21} X_x - d_{22} Y_y - d_{23} Z_z - d_{24} Y_z - d_{25} Z_x - d_{26} X_y + \kappa_2^F E_y \\
 P_z &= -d_{31} X_x - d_{32} Y_y - d_{33} Z_z - d_{34} Y_z - d_{35} Z_x - d_{36} X_y + \kappa_3^F E_z
 \end{aligned}$$

where  $x_x, y_y, z_z$  are the three longitudinal strains,  $y_z, z_x, x_y$  the three shearing strains,  $X_x, Y_y, Z_z$  the three longitudinal stresses  $Y_z, Z_x, X_y$  the three shearing stresses;  $P_x, P_y, P_z$  the  $x, y$  and  $z$  components of the polarization, and  $E_x, E_y, E_z$  the  $x, y$  and  $z$  components of the electric field.  $s_{11}^E, \dots, s_{66}^E$  are the 36 elastic compliances. The superscript  $E$  is added to show that they must be measured when the field  $E$  is zero or the crystal plated and short circuited. As shown from section C of this appendix they can be measured from the resonances of completely plated crystals. From the principle of conservation of energy it can be shown that there is the general relation between the elastic compliances

$$s_{ij}^E = s_{ji}^E \quad (\text{A.2})$$

so that the greatest number of compliance moduli is 21. In equation (A.1) the  $d_{ij}$  are the piezoelectric constants measured by observing the proportionality between the strains and the applied fields in the absence of external stresses.  $\kappa_i^F$  are the "free" susceptibilities of the crystals in the three space directions measured in the absence of stress. The susceptibilities are related to the "free" dielectric constants  $K_i^F$  by the equation

$$K_i^F = 1 + 4\pi\kappa_i^F \quad (\text{A.3})$$

In addition to these equations we have also that the charge per unit area  $Q$  on the surface is related to the field and polarization by

$$\begin{aligned}
 Q_x &= \frac{E_x}{4\pi} + P_x \\
 &= \frac{E_x K_1^F}{4\pi} - d_{11} X_x - d_{12} Y_y - d_{13} Z_z - d_{14} Y_z - d_{15} Z_x - d_{16} X_y \\
 &\quad \dots \dots \dots \quad (\text{A.4})
 \end{aligned}$$

$$\begin{aligned}
 Q_z &= \frac{E_z}{4\pi} + P_z \\
 &= \frac{E_z K_3^F}{4\pi} - d_{31} X_x - d_{32} Y_y - d_{33} Z_z - d_{34} Y_z - d_{35} Z_x - d_{36} X_y
 \end{aligned}$$

These equations hold for the most general type of crystal. In addition Voigt showed that if there was any symmetry existing in the crystal, a number of the constants were zero and certain relations existed between other constants. For example quartz has a trigonal symmetry about the  $Z$  or optic axis, and three digonal axes of symmetry (the three  $X$  or electrical axes) about which it is necessary to turn through an angle of  $180^\circ$  before the original pattern is restored. Voigt showed that by expressing the relations (A.1) in terms of rotated axes and imposing the symmetry conditions, the following relations existed between the elastic and piezoelectric coefficients

$$\begin{aligned}
 s_{15}^E &= s_{16}^E = s_{25}^E = s_{26}^E = s_{34}^E = s_{35}^E = s_{36}^E = s_{45}^E = s_{46}^E = 0 \\
 s_{22}^E &= s_{11}^E; \quad s_{23}^E = s_{13}^E; \quad s_{24}^E = -s_{14}^E; \quad s_{44}^E = s_{55}^E; \\
 & \quad s_{56}^E = 2s_{14}^E; \quad s_{66}^E = 2(s_{11}^E - s_{12}^E) \\
 d_{13} &= d_{15} = d_{16} = d_{21} = d_{22} = d_{23} = d_{24} = d_{31} = d_{32} \\
 & \quad = d_{33} = d_{34} = d_{35} = d_{36} = 0 \\
 d_{12} &= -d_{11}; \quad d_{25} = -d_{14}; \quad d_{26} = -2d_{11} \\
 \kappa_1^F &= \kappa_2^F
 \end{aligned} \tag{A.5}$$

Hence the relations between the stresses, strains, polarizations and fields for quartz reduce to the simpler forms

$$\begin{aligned}
 -x_x &= s_{11}^E X_x + s_{12}^E Y_y + s_{13} Z_z + s_{14}^E Y_z - d_{11} E_x \\
 -y_y &= s_{12}^E X_x + s_{11}^E Y_y + s_{13} Z_z - s_{14}^E Y_z + d_{11} E_x \\
 -z_z &= s_{13} X_x + s_{13} Y_y + s_{33} Z_z \\
 -y_z &= s_{14}^E X_x - s_{14}^E Y_y + s_{44}^E Y_z - d_{14} E_x \\
 -z_x &= s_{44}^E Z_z + 2s_{14}^E X_y + d_{14} E_y \\
 -x_y &= 2s_{14}^E Z_z + 2(s_{11}^E - s_{12}^E) X_y + 2d_{11} E_y \\
 Q_x &= \frac{E_x K_1^F}{4\pi} - d_{11} X_x + d_{11} Y_y - d_{14} Y_z \\
 Q_y &= \frac{E_y K_1^F}{4\pi} + d_{14} Z_z + 2d_{11} X_y \\
 Q_z &= \frac{E_z K_3}{4\pi}
 \end{aligned} \tag{A.6}$$

The superscripts have been left off the constants  $s_{13}$ ,  $s_{33}$  and  $K_3$  since it will be shown that their values are not affected by the way in which they are measured.

Equation (A.5) is not the only way of relating the elastic and electric quantities. For example if we substitute the values of the fields of the last three equations of (A.6) in the first six equations, we can write

$$\begin{aligned}
 -x_x &= s_{11}^Q X_x + s_{12}^Q Y_y + s_{13} Z_z + s_{14}^Q Y_z - g_{11} Q_x \\
 -y_y &= s_{12}^Q X_x + s_{11}^Q Y_y + s_{13} Z_z - s_{14}^Q Y_z + g_{11} Q_x \\
 -z_z &= s_{13} X_x + s_{13} Y_y + s_{33} Z_z \\
 -y_z &= s_{14}^Q X_x - s_{14}^Q Y_y + s_{44}^Q Y_z - g_{14} Q_x \\
 -z_x &= s_{44}^Q Z_x + 2s_{14}^Q X_y + g_{14} Q_y \\
 -x_y &= 2s_{14}^Q Z_x + 2(s_{11}^Q - s_{12}^Q) X_y + 2g_{11} Q_y \\
 E_x &= \frac{4\pi}{K_1^F} Q_x + g_{11} X_x - g_{11} Y_y + g_{14} Y_z \\
 E_y &= \frac{4\pi}{K_1^F} Q_y - g_{14} Z_x - 2g_{11} X_y \\
 E_z &= \frac{4\pi}{K_3} Q_z
 \end{aligned} \tag{A.7}$$

where

$$\begin{aligned}
 s_{11}^Q &= s_{11}^E - \frac{4\pi d_{11}^2}{K_1^F}; & s_{12}^Q &= s_{12}^E + \frac{4\pi d_{11}^2}{K_1^F}; & s_{14}^Q &= s_{14}^E - \frac{4\pi d_{11} d_{14}}{K_1^F} \\
 s_{44}^Q &= s_{44}^E - \frac{4\pi d_{14}^2}{K_1^F}; & g_{11} &= \frac{4\pi d_{11}}{K_1^F}; & g_{14} &= \frac{4\pi d_{14}}{K_1^F}
 \end{aligned}$$

The superscript  $Q$  is added to show that these are the elastic compliances that will be measured when the free charge on the surface is zero. These elastic constants are the ones measured when an unplated crystal is put in an airgap holder with a large air-gap since then no charge can flow to the surface of the crystal. The difference between the zero field and zero charge elastic constants for quartz is less than 1 per cent. For rochelle salt, however, they may differ by a factor of 4. For rochelle salt the principal piezoelectric constant  $d_{14}$  and the "free" dielectric constant  $K_1^F$  vary widely in value and phase angle with variations in temperature and frequency, whereas the piezoelectric constant  $g_{14}$  which is proportional to the ratio of these two is nearly a constant for all frequencies and temperatures, so that the formulation of equation (A.7) is more advantageous than that of equation (A.6). For quartz, however, both forms are reasonably constant. Furthermore the elastic constants of equation (A.6) are those for a plated crystal which are usually the ones of interest for a crystal employed in an oscillator or filter. Hence this formulation has been used in this appendix.

Both the formulation of (A.6) and (A.7) can be expressed in terms of the strains rather than the stresses. Since these are useful forms and are used later in this appendix, they are given below. Equations (A.8) are obtained directly from equations (A.6) by solving them simultaneously to replace the strain by the stress, while equations (A.10) are obtained in the same way from equations (A.7).

$$\begin{aligned}
 -X_x &= c_{11}^E x_x + c_{12}^E y_y + c_{13} z_z + c_{14}^E y_z - e_{11} E_x \\
 -Y_y &= c_{12}^E x_x + c_{11}^E y_y + c_{13} z_z - c_{14}^E y_z + e_{11} E_x \\
 -Z_z &= c_{13} x_x + c_{13} y_y + c_{33} z_z \\
 -Y_z &= c_{14}^E x_x - c_{14}^E y_y + c_{44}^E y_z - e_{14} E_x \\
 -Z_x &= c_{44}^E z_x + c_{14}^E x_y + e_{14} E_y \\
 -X_y &= c_{14}^E z_x + \left( \frac{c_{11}^E - c_{12}^E}{2} \right) x_y + e_{11} E_y \quad (\text{A.8}) \\
 Q_x &= \frac{E_x}{4\pi} + P_x = \frac{E_x K_1^C}{4\pi} + e_{11} x_x - e_{11} y_y + e_{14} y_z \\
 Q_y &= \frac{E_y}{4\pi} + P_y = \frac{E_y K_1^C}{4\pi} - e_{14} z_x - e_{11} x_y \\
 Q_z &= \frac{E_z}{4\pi} + P_z = \frac{E_z K_3}{4\pi}
 \end{aligned}$$

where the relations for the elastic constants are

$$\begin{aligned}
 2c_{11}^E &= \frac{s_{33}^E}{\alpha} + \frac{s_{44}^E}{\beta}; & 2c_{12}^E &= \frac{s_{33}^E}{\alpha} - \frac{s_{44}^E}{\beta}; & c_{13} &= \frac{-s_{13}}{\alpha}; \\
 c_{14}^E &= \frac{-s_{14}}{\beta}; & c_{33} &= \frac{s_{11}^E + s_{12}^E}{\alpha}; & c_{44}^E &= \frac{s_{11}^E - s_{12}^E}{\beta}; \\
 c_{66}^E &= \frac{c_{11}^E - c_{12}^E}{2} = \frac{s_{44}^E}{2\beta}; & \alpha &= s_{33}(s_{11}^E + s_{12}^E) - 2s_{13}^2; \\
 \beta &= s_{44}(s_{11}^E - s_{12}^E) - 2s_{14}^{E2}.
 \end{aligned}$$

Conversely we can also write the useful relation

$$\begin{aligned}
 2s_{11}^E &= \frac{c_{33}^E}{\alpha'} + \frac{c_{44}^E}{\beta'}; & 2s_{12}^E &= \frac{c_{33}^E}{\alpha'} - \frac{c_{44}^E}{\beta'}; \\
 s_{13} &= \frac{-c_{13}}{\alpha'}; & s_{14}^E &= \frac{-c_{14}^E}{\beta'}; & s_{33} &= \frac{c_{11}^E + c_{12}^E}{\alpha'}; \\
 s_{44}^E &= \frac{c_{11}^E - c_{12}^E}{\beta'}; & s_{66}^E &= 2(s_{11}^E - s_{12}^E) = \frac{2c_{44}^E}{\beta'}; \\
 \alpha' &= c_{33}(c_{11}^E + c_{12}^E) - 2c_{13}^2; & \beta' &= c_{44}(c_{11}^E - c_{12}^E) - 2c_{14}^{E2}.
 \end{aligned}$$

For the piezoelectric constants

$$e_{11} = d_{11}(c_{11}^E - c_{12}^E) + d_{14}c_{14}^E; \quad e_{14} = 2d_{11}c_{14}^E + d_{14}c_{44}^E;$$

and conversely

$$-d_{11} = e_{11}(s_{11}^E - s_{12}^E) + e_{14}s_{14}^E; \quad -d_{14} = 2e_{11}s_{14}^E + e_{14}s_{44}^E.$$

The dielectric constant  $K_1^C$  denotes the clamped dielectric constant, i.e., the constant measured when the crystal is free from strain. This is related to the free dielectric constant  $K_1^F$  by the equation

$$K_1^C = K_1^F - 4\pi[d_{14}e_{14} + 2d_{11}e_{11}]. \quad (\text{A.9})$$

In a similar way if we solve equations (A.7) simultaneously, for the stresses in terms of the strains, we have

$$\begin{aligned} -X_x &= c_{11}^Q x_x + c_{12}^Q y_y + c_{13} z_z + c_{14}^Q y_z - f_{11} Q_x; \\ -Y_y &= c_{12}^Q x_x + c_{11}^Q y_y + c_{13} z_z - c_{14}^Q y_z + f_{11} Q_x; \\ -Z_z &= c_{13} x_x + c_{13} y_y + c_{33} z_z; \\ -Y_z &= c_{14}^Q x_x - c_{14}^Q y_y + c_{44}^Q y_z - f_{14} Q_x; \\ -Z_x &= c_{44}^Q z_z + c_{14}^Q x_y + f_{14} Q_y; \\ -X_y &= c_{14}^Q z_z + \left( \frac{c_{11}^Q - c_{12}^Q}{2} \right) x_y + f_{11} Q_y; \\ E_x &= \frac{4\pi}{K_1^C} Q_x - f_{11} x_x + f_{11} y_y - f_{14} y_z; \\ E_y &= \frac{4\pi}{K_1^C} Q_y + f_{14} z_z + f_{11} x_y; \\ E_z &= \frac{4\pi}{K_3} Q_z. \end{aligned} \quad (\text{A.10})$$

where the  $c^Q$  constants are related to the  $s^Q$  constants as in equation (A.8). The piezoelectric relations are

$$f_{11} = g_{11}(c_{11}^Q - c_{12}^Q) + g_{14}c_{14}^Q; \quad f_{14} = 2g_{11}c_{14}^Q + g_{14}c_{44}^Q;$$

or conversely

$$-g_{11} = f_{11}(s_{11}^Q - s_{12}^Q) + e_{14}s_{14}^Q; \quad -g_{14} = 2f_{11}s_{14}^Q + f_{14}s_{44}^Q;$$

while the dielectric relation between the free and clamped crystal

$$\frac{4\pi}{K_1^F} = \frac{4\pi}{K_1^C} - (g_{14}f_{14} + 2g_{11}f_{11}). \quad (\text{A.11})$$

Equations (A.10) might also have been obtained directly from equations (A.8) by substituting the charges from the last three equations in terms of the fields. This substitution yields the additional relations

$$\begin{aligned}
 c_{11}^Q &= c_{11}^E + \frac{4\pi e_{11}^2}{K_1^C}; & c_{12}^Q &= c_{12}^E - \frac{4\pi e_{11}^2}{K_1^C}; & c_{13}^Q &= c_{13}^E; \\
 c_{14}^Q &= c_{14}^E + \frac{4\pi e_{11} e_{14}}{K_1^C}; & c_{33}^Q &= c_{33}^E; \\
 c_{44}^Q &= c_{44}^E + \frac{4\pi e_{14}^2}{K_1^C}; & c_{66}^Q &= \frac{c_{11}^Q - c_{12}^Q}{2} = \frac{c_{11}^E - c_{12}^E + \frac{8\pi e_{11}^2}{K_1^C}}{2}; \\
 f_{11} &= \frac{4\pi}{K_1^C} e_{11}; & f_{14} &= \frac{4\pi}{K_1^C} e_{14}.
 \end{aligned} \tag{A.12}$$

#### (A.2). VALUES OF THE ELASTIC AND PIEZOELECTRIC CONSTANTS

The first and one of the best determinations of the elastic constants of quartz was made by Voigt. Using static deformations of unplated crystals he determined the elastic constants to be

$$\begin{aligned}
 c_{11} &= 85.1 \times 10^{10} \text{ dynes/cm}^2; & c_{12} &= 6.95 \times 10^{10}; \\
 c_{13} &= 14.1 \times 10^{10}; & c_{14} &= 16.8 \times 10^{10} \\
 c_{33} &= 105.3 \times 10^{10}; & c_{44} &= 57.1 \times 10^{10}; \\
 c_{66} &= \left( \frac{c_{11} - c_{12}}{2} \right) = 39.1 \times 10^{10}
 \end{aligned} \tag{A.13}$$

From these the moduli of compliance can be calculated and are

$$\begin{aligned}
 s_{11} &= 129.8 \times 10^{-14} \text{ cm}^2/\text{dyne}; & s_{12} &= -16.6 \times 10^{-14}; \\
 s_{13} &= -15.2 \times 10^{-14}; & s_{14} &= -43.1 \times 10^{-14}; \\
 s_{33} &= 99.0 \times 10^{-14}; & s_{44} &= 200.5 \times 10^{-14}; \\
 s_{66} &= 2(s_{11} - s_{12}) = 292.8 \times 10^{-14}.
 \end{aligned} \tag{A.14}$$

Whether these are zero field or zero charge constants is not known. If they were measured in a room with high humidity, the polarization produced by strain would soon be annulled by a current flow through the leakage resistance of the adsorbed moisture, and the constants would be  $c_{ij}^E$  or  $s_{ij}^E$ . On the other hand if the displacements were measured in a very dry room, the leakage resistance is very small and it may take hours to annul the polarization through a leakage current flow. In that case the constants measured

would be  $c_{ij}^0$  or  $s_{ij}^0$ . In any case the difference was probably less than the accuracy of measurement.

Later measurements by Perrier and Mandrot for two of the constants  $s_{11}$  and  $s_{33}$  give the values

$$s_{11} = 127.3 \times 10^{-14}; \quad s_{33} = 97 \times 10^{-14} \quad (\text{A.15})$$

By using the measured resonance frequencies of known modes of motion, the uncertainty of the type of elastic constant can be removed, for the alternations occur so fast that the leakage resistance has little effect. If a crystal is lightly plated, it is shown in the next section that the resonant frequency of a length vibrating bar will be determined by the zero field elastic constants  $s_{ij}^E$ . On the other hand if an unplated crystal is measured in an air gap holder with a large air gap it has been shown that<sup>1</sup> the frequency measured will be determined by the zero charge elastic constants  $s_{ij}^0$  or  $c_{ij}^0$ . A careful measurement of the elastic constants of quartz has recently been made by Atanasoff and Hart<sup>2</sup>. Using thickness modes for

<sup>1</sup> The resonances of length vibrating crystals have been discussed by Cady, "The Piezo-electric Resonator and The Effect of Electrode Spacing on Frequency," *Physics*, Vol. 7, No. 7, July 1936, pages 237-259; and by the writer, "Dynamic Measurement of The Constants of Rochelle Salt," *Phys. Rev.*, Vol. 55, pages 775-789, April 15, 1939; while the resonances of thickness vibrating crystals have been discussed by Cady (above paper) and Lawson "The Vibration of Piezoelectric Plates," *Phys. Rev.*, Vol. 62, July 1, 1942, pp. 71-76. For a length vibrating crystal Cady shows that the resonant frequency for no air gap (plated crystal) is controlled by the constant  $1/s_{11}^E$ . For a crystal with a large air gap, the frequency is controlled by the constant.

$$1/s_{11}^E + 4\pi d_{11}^2/K_1^E s_{11}^{E2} = 1/s_{11}^0.$$

Starting with equations of the form (A.10), the writer showed that the frequency of a bar in an air gap holder would be controlled by the constant  $1/s_{11}^0$ , while the frequency of a plated crystal is determined by

$$s_{11}^0 / \left( 1 - \frac{d_{11}^2 4\pi}{K_1^C s_{11}^0} \right) = s_{11}^E.$$

For a thickness vibrating crystal for which the field is applied in the direction of wave propagation, Cady and Lawson find that the resonant frequency is controlled by the elastic constant

$$c^* = c_{11}^E + \frac{4\pi e_{11}^2}{K_1^C} \left[ 1 - \frac{8}{\pi^2 \left[ 1 + K_1^C \left( \frac{D}{t} - 1 \right) \right]} \right]$$

where  $D$  is the total separation between electrodes and  $t$  the thickness of the crystal. When the separation is infinite, the controlling elastic constant is  $c_{11}^E + 4\pi e_{11}^2/K_1^C$  which, from equation (A.12) is  $c_{11}^0$ . When the air gap is zero or  $D = t$ , the controlling constant is

$$c_{11}^E + \frac{4\pi e_{11}^2}{K_1^C} \left( 1 - \frac{8}{\pi^2} \right)$$

which, for all practical purposes, can be taken as  $c_{11}^E$  for quartz.

<sup>2</sup> "Dynamical Determination of the Elastic Constants and their Temperature Coefficients for Quartz," *Phys. Rev.*, Vol. 59, No. 1 (85-96), Jan. 1, 1941.

relatively thick pieces of quartz, and determining the asymptotic value for high order harmonics, they obtained the elastic constants

$$\begin{aligned} c_{11} &= 87.55 \times 10^{10} \text{ dynes/cm}^2; & c_{12} &= 6.07 \times 10^{10}; & c_{13} &= 13.3 \times 10^{10}; \\ c_{14} &= -c_{24} = 17.25 \times 10^{10}; & c_{33} &= 106.8 \times 10^{10}; & c_{44} &= 57.19 \times 10^{10}. \end{aligned} \quad (\text{A.16})$$

In addition they came to the conclusion that  $c_{56}$  had a value of  $18.4 \times 10^{10}$ , which was different from the value of  $c_{14}$  as required by theory. Their measurements were made with high harmonics in air gap holders so that the values measured should determine the  $c_{ij}^Q$  constant. To explain the discrepancy found, Lawson<sup>3</sup> has suggested that the  $c_{ij}^Q$  constants

$$c_{ij}^Q = c_{ij}^R + 4\pi e_{1i}e_{1j}/K_1^C \quad (\text{A.17})$$

do not obey the same symmetry relations as the  $c_{ij}^R$  constants. This suggestion does not seem to be borne out by equations (A.10), from which the symmetry relations of the  $c_{ij}^Q$  constants can be determined. If we start with a generalized form of these equations applicable to any crystal and apply the symmetry relations for quartz, we find that it is still necessary to satisfy the symmetry relations between the constants found previously and in particular

$$c_{56}^Q = c_{14}^Q \quad (\text{A.18})$$

In order to investigate this matter further, and to obtain more reliable values of the elastic constants, an analysis has been made of a number of measurements previously obtained for oriented crystals. In particular two families of oriented crystals were investigated. One family was a set of oriented  $X$  cut crystals vibrating longitudinally. They were cut with their major faces normal to the  $X$  axis and with their lengths at angles  $A_2$  of from  $+43^\circ$  to  $-79^\circ$  with respect to the  $Y$  or mechanical axis. They were oriented similarly to the  $+5^\circ$  and  $-18.5^\circ$  filter crystals shown by Fig. 1.9. When these crystals are 7 to 10 times as long as they are wide or thick it has been shown previously<sup>4</sup> that their length resonances are determined very accurately by the equation

$$f_R = \frac{1}{2\ell_y} \sqrt{\frac{1}{\rho s_{22}^R}} \quad (\text{A.19})$$

where  $\ell_y$  is the length of the crystal,  $\rho$  the density and  $s_{22}^R$  the inverse of Young's Modulus along the length for a plated crystal. This is related to the angle of cut  $A_2$  by the equation

$$\begin{aligned} s_{22}^R &= s_{11}^R \cos^4 A_2 + s_{33}^R \sin^4 A_2 + 2s_{14}^R \cos^3 A_2 \sin A_2 \\ &\quad + (2s_{13} + s_{44}^R) \sin^2 A_2 \cos^2 A_2 \end{aligned} \quad (\text{A.20})$$

<sup>3</sup> A. W. Lawson, *Phys. Rev.*, 59, 838 (1941).

<sup>4</sup> "Electrical Wave Filters Employing Quartz Crystals as Elements," W. P. Mason, *B. S. T. J.*, Vol. XIII, pp. 405-452, July 1934. See Figs. 25, 31 and 32.



Since the resonant frequency of the plated crystal was measured, it was the zero potential elastic constant that was determined. These crystals were lightly plated with aluminum and it had been previously shown that the added plating would affect the frequency by considerably less than 0.1 per cent. The crystal orientations, their dimensions, the frequency constants and the values of  $s_{22}^E$  are shown by Table I.

These measured variations satisfy equation (A.20) for the variation of  $s_{22}^E$  with angle very well if we take

$$\begin{aligned} s_{11}^E &= 127.9 \times 10^{-14} \text{ cm}^2/\text{dyne}; & s_{33} &= 95.6 \times 10^{-14}; \\ s_{14}^E &= -44.6 \times 10^{-14}; & & \\ s_{44}^E + 2s_{13} &= 175.8 \times 10^{-14}. \end{aligned} \quad (\text{A.21})$$

TABLE I

Angle of Cut, $A_2$	Dimension, mm			Resonant Frequency 25°C	Frequency Constant KC cms	Value of $s_{22}^E$
	Length	Width	Thickness			
-79.5°	24.03	2.50	.502	130,700	314.1	95.6 × 10 <sup>-14</sup> cm <sup>2</sup> /dyne
-18.5°	20.00	2.50	.502	127,710	255.4	144.5
-13.14°	19.99	2.97	.505	128,390	256.8	143.0
-12.33	19.98	2.95	.500	128,590	257.0	142.7
-5.6	20.02	2.92	.500	132,130	264.5	134.7
-1.4	20.03	3.02	.502	134,050	269.2	130.2
-.9°	19.97	2.99	.502	135,240	270.5	128.9
+ .36°	20.03	3.03	.508	135,890	272.0	127.5
+ .54	19.96	2.98	.506	135,920	272.1	127.3
+ 1.44	20.02	2.98	.505	136,890	274.0	125.7
+ 2.61	19.97	3.00	.505	138,400	276.5	123.3
+ 4.05	19.95	2.97	.510	139,900	279.0	121.2
+11.8	19.11	3.01	.500	154,600	295.4	108.1
+18.0	20.02	2.95	.500	155,380	311.1	97.5
+42.6	20.00	2.95	.500	174,750	349.5	77.25

This gives three of the constants directly, and a relation between two more. To obtain the remaining constants and to test out the hypothesis that there are seven elastic constants rather than six, use has been made of measurements made for thickness vibrating shear crystals obtained by rotating one edge about the  $X$  axis. These are the  $AT$  and  $BT$  series shown by Fig. 1.9. As shown by a former paper<sup>5</sup>, the frequency of such crystals depends on the edge dimensions as well as the thickness dimensions. However, as the edge dimensions become large compared to the thickness dimension the principal frequency approaches an asymptotic value which is taken as that for the infinite plate. For the  $AT$ ,  $BT$  and  $Y$  cut crystals these asymptotic values have been determined to have the values shown by Table II.

<sup>5</sup> "Low Temperature Coefficient Quartz Crystals," *B. S. T. J.*, Vol. XIX, pp. 74-93, Jan. 1940. See Fig. 5.

If we make the assumption that there are seven elastic constants and  $c_{56}^E$  differs from  $c_{14}^E$ , the frequency of this series of crystals will be<sup>5</sup>

$$f = \frac{1}{2\ell} \sqrt{\frac{c_{66}^E}{\rho}} \quad \text{where } c_{66}^E = c_{66}^E \cos^2 A_2 + c_{44}^E \sin^2 A_2 - c_{56}^E \sin 2A_2 \quad (\text{A.22})$$

The determination for the *Y* cut gives directly

$$c_{66}^E = 40.5 \times 10^{10} \text{ dynes per square cm.} \quad (\text{A.23})$$

The other two cuts give the values

$$c_{56}^E = 18.2 \times 10^{10}; \quad c_{44}^E = 58.65 \times 10^{10} \quad (\text{A.24})$$

To test out the hypothesis that  $c_{56}^E$  differs from  $c_{14}^E$  or  $s_{56}^E$  from  $2s_{14}^E$  we can make use of equation (A.8) writing  $c_{56}^E$  in place of  $c_{14}^E$ . Then solving these equations simultaneously we find

$$s_{44}^E = \frac{c_{66}^E}{(c_{44}^E c_{66}^E - c_{56}^{E2})}; \quad s_{56}^E = \frac{-c_{56}^E}{(c_{44}^E c_{66}^E - c_{56}^{E2})}; \quad s_{66}^E = \frac{c_{44}^E}{(c_{44}^E c_{66}^E - c_{56}^{E2})} \quad (\text{A.25})$$

TABLE II

Crystal	Angle of Cut $A_2$	Asymptotic Frequency constant KC mms	Value of $c_{66}^E$
<i>AT</i>	+35° 15'	1661.5	$29.39 \times 10^{10}$ dynes/cm <sup>2</sup>
<i>Y</i> Cut	0	1954	40.50
<i>BT</i>	-49°	2549	68.86

Substituting in the values from (A.23) and (A.24) we find

$$s_{44}^E = 197.8 \times 10^{-14} \text{ cm}^2/\text{dyne}; \quad s_{56}^E = -89.0 \times 10^{-14}; \quad (\text{A.26})$$

$$s_{66}^E = 2(s_{11}^E - s_{12}^E) = 286.5 \times 10^{-14}.$$

Comparing the value of  $s_{56}^E$  with  $2s_{14}^E$  given in equation (A.21) we see that they are equal within the experimental error, so that these measurements do not indicate that there are seven elastic constants but only the customary six. Using these values all the elastic constants can be evaluated as shown by Table III.

Measurements have also been made to determine accurately the piezoelectric constants. This was done by using the ratios of capacities of two standard rotated *X* cut crystals for which these ratios have been accurately determined. As shown by section C of this appendix, the ratio of capacities  $r$  of a crystal is related to the piezoelectric constant  $d_{12}^E$ , the elastic constant  $s_{22}^E$ , and the free dielectric constant  $K_1^E$  by the equation

$$r = \text{ratio of capacities} = \frac{\pi^2}{8} \left( \frac{1 - k^2}{k^2} \right) \quad (\text{A.27})$$

where  $k$  the electromechanical coupling is given by

$$k = d_{12}' \sqrt{\frac{4\pi}{K_1^F s_{22}^{E'}}}. \quad (\text{A.28})$$

The two crystal cuts and their constants are given in Table IV. Only the numerical value and not the sign are determined for  $d_{12}'$ .

TABLE III

Elastic Compliance Moduli	Elastic Stiffness Moduli
$s_{11}^E = 127.9 \times 10^{-14}$ cm <sup>2</sup> /dyne	$c_{11}^E = 86.05 \times 10^{10}$ dynes/cm <sup>2</sup>
$s_{12}^E = -15.35$	$c_{12}^E = 5.05$
$s_{13} = -11.0$	$c_{13} = 10.45$
$s_{14}^E = -44.6$	$c_{14}^E = 18.25$
$s_{33} = 95.6$	$c_{33} = 107.1$
$s_{44}^E = 197.8$	$c_{44}^E = 58.65$
$s_{66}^E = 2(s_{11}^E - s_{12}^E) = 286.5$	$c_{66}^E = \frac{c_{11}^E - c_{12}^E}{2} = 40.5$

TABLE IV

Angle of Cut, $A_2$	Ratio of Capacities	Value of $s_{22}^{E'}$	Value of $K_1^F$	Value of $d_{12}'$
$-18.5^\circ X$ cut	137	144.5	4.58	$6.85 \times 10^{-8}$
$0^\circ X$ cut	125	127.9	4.58	$6.76 \times 10^{-8}$

TABLE V

Piezoelectric constant	Value in cgs electrostatic units	Piezoelectric constant	Value in cgs electrostatic units
$d_{11}$	$-6.76 \times 10^{-8}$	$g_{11}$	$-18.55 \times 10^{-8}$
$d_{14}$	$2.56 \times 10^{-8}$	$g_{14}$	$7.02 \times 10^{-8}$
$e_{11}$	$-5.01 \times 10^4$	$f_{11}$	$-13.85 \times 10^4$
$e_{14}$	$-.97 \times 10^4$	$f_{14}$	$-2.68 \times 10^4$

The variation of  $d_{12}'$  as a position of angle has been shown to be<sup>6</sup>

$$d_{12}' = -\frac{1}{2}[d_{11}(1 + \cos 2A_2) + d_{14} \sin 2A_2] \quad (\text{A.29})$$

The two values of  $d_{12}'$  of table IV are satisfied by

$$d_{11} = -6.76 \times 10^{-8}; \quad d_{14} = +2.56 \times 10^{-8} \quad (\text{A.30})$$

<sup>6</sup> See "Electrical Wave Filters Employing Quartz Crystals as Elements," W. P. Mason, B. S. T. J., Vol. XIII, 405 (July 1934).

From these values and the elastic constants of Table III we can calculate all the different forms of the piezoelectric constants. These are given in Table V.

### (A.3). DERIVATION OF EQUIVALENT CIRCUIT OF CRYSTAL

The electrical impedance and electrical equivalent circuit for a fully plated crystal can be derived from the piezoelectric relations of equation (A.6) taken together with Newton's law of motion

$$F_y = ma = (\rho dx dy dz) \frac{d^2\xi}{dt^2} \quad (\text{A.31})$$

where  $m$  is mass of an elementary volume  $dx dy dz$ ,  $a$  the acceleration, and  $\xi$  is the displacement of the element in the  $y$  direction. If we consider a long thin  $X$  cut crystal with its length in the  $y$  direction, the piezoelectric relations of interest are

$$\begin{aligned} -y_y &= s_{12}^E X_x + s_{11}^E Y_y + s_{13} Z_z - s_{14}^E Y_z + d_{11} E_x; \\ Q_x &= \frac{E_x K_1^P}{4\pi} - d_{11} X_x + d_{11} Y_y - d_{14} Y_z. \end{aligned} \quad (\text{A.32})$$

For a long thin crystal with its long dimension in the  $Y$  direction we can set

$$X_x = Z_z = Y_z = 0 \quad (\text{A.33})$$

This follows since the crystal is free from external forces, and hence these stresses on the edges of the crystal must be zero. On account of the small  $x$  and  $z$  dimensions, the rate of change of these stresses with  $x$  or  $z$  will have to be high in order that the stresses shall differ appreciably from zero, and there are no mechanical strains causing a high stress gradient. Then for a long thin bar the piezoelectric equations can be written

$$\begin{aligned} -y_y &= s_{11}^E Y_y + d_{11} E_x; \\ Q_x &= \frac{E_x K_1^P}{4\pi} + d_{11} Y_y. \end{aligned} \quad (\text{A.34})$$

Let us next consider a small cross section of the crystal with a dimension  $dy$  along the crystal length. The total force on the section is a resultant of the difference in stresses on the two faces or equal to

$$\ell_w \ell_t [Y_{y_1} - Y_{y_2}] = -\ell_w \ell_t \frac{\partial Y_y}{\partial y} dy = F_y \quad (\text{A.35})$$

where  $Y_y$  the stress is considered as a compressional force acting on the faces of the element. By Newton's law of motion (A.31) we have

$$-\ell_w \ell_t dy \frac{\partial Y_y}{\partial y} = \ell_w \ell_t dy \rho \frac{d^2\xi}{dt^2} \quad \text{or} \quad \frac{\partial Y_y}{\partial y} = -\rho \frac{d^2\xi}{dt^2} \quad (\text{A.36})$$

For a completely plated crystal such as we are considering, the potential gradient  $E_x$  will be independent of the  $y$  direction, since any charge distribution will be equalized with the speed of light which is much higher than the speed of sound in the crystal. Then equation (A.34) when differentiated by  $y$  becomes

$$-\frac{\partial Y_y}{\partial y} = -\frac{\partial^2 \xi}{\partial y^2} = s_{11}^E \frac{\partial y_y}{\partial y}. \quad (\text{A.37})$$

Introducing equation (A.36), the equation of motion for a plated crystal becomes

$$\frac{\partial^2 \xi}{\partial y^2} = s_{11}^E \rho \frac{d^2 \xi}{dt^2}. \quad (\text{A.38})$$

For simple harmonic motion the variation of  $\xi$  with time can be written in the usual form

$$\xi = \xi e^{i\omega t}, \quad (\text{A.39})$$

so that for simple harmonic motion equation (A.38) becomes

$$\frac{d^2 \xi}{dy^2} - \omega^2 s_{11}^E \rho \xi = \frac{d^2 \xi}{dy^2} - \frac{\omega^2}{v^2} \xi = 0 \quad (\text{A.40})$$

where  $v$  the velocity of sound in the plated crystal is given by the formula

$$v^2 = \frac{1}{\rho s_{11}^E}. \quad (\text{A.41})$$

A solution of equation (A.40) with two arbitrary boundary conditions is

$$\xi = A \cos \frac{\omega}{v} y + B \sin \frac{\omega y}{v}. \quad (\text{A.42})$$

To determine the constants  $A$  and  $B$ , use is made of equation (A.34). Differentiating (A.42)

$$-\frac{\partial \xi}{\partial y} = -y_y = \frac{\omega}{v} \left[ A \sin \frac{\omega}{v} y - B \cos \frac{\omega y}{v} \right] = s_{11}^E Y_y + d_{11} E_x. \quad (\text{A.43})$$

When  $y = 0$  and  $y = \ell$  the bar length

$$Y_y = Y_{y_1} \quad \text{and} \quad Y_y = Y_{y_2} \quad (\text{A.44})$$

provided the crystal is driving a load. For most electrical cases the only load driven is an air load and this is usually very small so that it is customary to set  $Y_{y_1} = Y_{y_2} = 0$ . Under these conditions

$$-\frac{\omega}{v} B = d_{11} E_x \quad \text{and} \quad \frac{\omega}{v} \left[ A \sin \frac{\omega \ell}{v} - B \cos \frac{\omega \ell}{v} \right] = d_{11} E_x. \quad (\text{A.45})$$

Solving these equations for  $A$  and  $B$  and substituting in (A.43) we have

$$-y_y = d_{11} E_x \left[ \tan \frac{\omega \ell}{2v} \sin \frac{\omega y}{v} + \cos \frac{\omega y}{v} \right] = s_{11}^E Y_y + d_{11} E_x$$

or

$$Y_y = -\frac{d_{11} E_x}{s_{11}^E} \left[ 1 - \frac{\cos \frac{\omega(y - \ell/2)}{v}}{\cos \frac{\omega \ell}{2v}} \right]. \quad (\text{A.46})$$

The electrical impedance measured at the terminals of a plated crystal is then determined by substituting the value of  $Y_y$  in the last of equations (A.34) and integrating the charge  $Q$  over the whole surface. The current into the crystal is then

$$i = j\omega Q = j\omega \ell_w \int_0^\ell E_x \left[ \frac{K_1^F}{4\pi} - \frac{d_{11}^2}{s_{11}^E} \left( 1 - \frac{\cos \omega(y - \ell/2)}{\cos \frac{\omega \ell}{2v}} \right) \right] dy$$

$$= j\omega E_x \ell_w \ell \left[ \frac{K_1^F}{4\pi} - \frac{d_{11}^2}{s_{11}^E} \left( 1 - \frac{\tan \frac{\omega \ell}{2v}}{\frac{\omega \ell}{2v}} \right) \right] \quad (\text{A.47})$$

$$= j\omega E_x \ell \ell \left[ \frac{K_1^{LC}}{4\pi} + \frac{d_{11}^2}{s_{11}^E} \frac{\tan \frac{\omega \ell}{2v}}{\frac{\omega \ell}{2v}} \right]$$

where  $K_1^{LC} = K_1^F - \frac{4\pi d_{11}^2}{s_{11}^E}$  is called the longitudinally clamped dielectric constant, i.e. the dielectric constant that would be measured if we suppress the longitudinal strain along the  $y$  axis but not the other strains. The admittance of the crystal then is

$$\frac{i}{E} = \frac{i}{E_x \ell_t} = \frac{j\omega \ell_w \ell}{\ell_t} \left[ \frac{K_1^{LC}}{4\pi} + \frac{d_{11}^2}{s_{11}^E} \frac{\tan \frac{\omega \ell}{2v}}{\frac{\omega \ell}{2v}} \right]. \quad (\text{A.48})$$

This consists of two terms which represent parallel branches in the equivalent circuit. One of these is the capacitance

$$C_0 = \frac{\ell_w \ell K_1^{LC}}{4\pi \ell_t} \text{ cgs units} = \frac{\ell_w \ell K_1^{LC}}{4\pi \ell_t 9 \times 10^{11}} \text{ farads} \quad (\text{A.49})$$

The other branch contains the impedance

$$\frac{-j\ell_i \left[ \frac{s_{11}^E}{d_{11}^2} \frac{\omega\ell}{2v} \right]}{\omega\ell_w \ell \left[ \frac{s_{11}^E}{d_{11}^2} \tan \frac{\omega\ell}{2v} \right]} \text{ cgs units} = \frac{-j\ell_i s_{11}^E \frac{\omega\ell}{2v} \times 9 \times 10^{11}}{\omega\ell_w \ell d_{11}^2 \tan \frac{\omega\ell}{2v}} \text{ ohms} \quad (\text{A.50})$$

This branch will have a zero impedance or will resonate when the tangent is infinite or when

$$\frac{2\pi f_R \ell}{2v} = \frac{\pi}{2} \text{ or } f_R = \frac{v}{2\ell} = \frac{1}{2\ell\sqrt{\rho s_{11}^E}} \quad (\text{A.51})$$

Hence for a fully plated crystal it is the zero field elastic constant that determines the resonant frequency.

Near this resonant frequency, the impedance of equation (A.50) can be represented by a series capacitance and inductance having the values

$$C_1 = \frac{\ell_w \ell}{\ell_i} \frac{8}{\pi^2} \frac{d_{11}^2}{s_{11}^E \times 9 \times 10^{11}}, \quad L_1 = \frac{\rho s_{11}^{E^2} \ell \ell_i \times 9 \times 10^{11}}{8\ell_w d_{11}^2} \quad (\text{A.52})$$

Taking the ratio between  $C_0$  and  $C_1$  we have

$$\frac{C_0}{C_1} = r = \frac{\pi^2 \left( \frac{K_1^{LC} s_{11}^E}{4\pi d_{11}^2} \right)}{8 \left( \frac{4\pi d_{11}^2}{K_1^F s_{11}^E} \right)} = \frac{\pi^2 \left( 1 - \frac{4\pi d_{11}^2}{s_{11}^E K_1^F} \right)}{8 \left( \frac{1 - k^2}{k^2} \right)} \quad (\text{A.53})$$

where  $k$  the coefficient of electromechanical coupling is equal to

$$k = d_{11} \sqrt{\frac{4\pi}{K_1^F s_{11}^E}} \quad (\text{A.54})$$

These values are used in equations (A.27) and (A.28) to evaluate the piezoelectric constants of quartz.

#### A.4. USE OF VOIGT'S RELATIONS IN LOCATING REGIONS OF LOW TEMPERATURE COEFFICIENT CRYSTALS FOR SIMPLE MODES OF MOTION

In Section 1.5 of the text, the statement is made that all longitudinally vibrating crystals of quartz have a zero or negative temperature coefficients. This can be proved from Voigt's relations for quartz and a knowledge of the temperature coefficients of the six elastic constants of quartz. Since the same method can be used to locate the regions of low temperature coefficient for other simple modes of motion a short discussion of the method is given here.

The Voigt relations given in equation (A.6) give the values of the piezo-

electric and elastic constants for crystals with their three edge dimensions along the three crystallographic axes. Most low-coefficient crystals, however, are oriented crystals with one or more of their edges lying along directions not parallel to the crystallographic axes. The theory of elasticity, however, provides methods for calculating the values of the constants for rotated axes. If the rotated axes  $X'$ ,  $Y'$ ,  $Z'$  are related to the crystallographic axes  $X$ ,  $Y$ , and  $Z$  by the relation

$$\begin{array}{l} X' \\ Y' \\ Z' \end{array} \begin{array}{c} \left| \begin{array}{ccc} \ell_1 & m_1 & n_1 \\ \ell_2 & m_2 & n_2 \\ \ell_3 & m_3 & n_3 \end{array} \right. \end{array} \quad (\text{A.55})$$

where  $\ell_1, \dots, n_3$  are the direction cosines between the axes indicated, the theory of elasticity provided relations between the stresses of the rotated axes and the stresses of the crystallographic axes, between the strains of the rotated axes and the strains of the crystallographic axes, and between the field, polarizations, or charges of the rotated axes and the same quantities for the crystallographic axes. Then if we express<sup>7</sup> the relation between the stress, strain and fields for the rotated axes, the elastic and piezoelectric constants are determined.

Two shorthand methods are also available for calculating the constants of rotated crystals. One method<sup>8</sup> is the matrix method which is based upon the fact that relations in (A.6) can be expressed in a matrix equation

$$-\epsilon = s^E X + dE \quad (\text{A.56})$$

where  $\epsilon$  are the strain components,  $X$  the stress components,  $s^E$  the elastic compliance matrix,  $d$  the piezoelectric matrix and  $E$  the field components. By applying the rules of matrix multiplication the  $s$  and  $d$  matrices can be transformed to rotated axes having the direction cosines of equation (A.57) with respect to the crystallographic axes. The other method is the method of tensor analysis. Equations (A.6) can be expressed in the form<sup>9</sup>

$$-\epsilon_{ij} = s_{ij\alpha\beta}^E X_{\alpha\beta} + d_{ij\nu} E_\nu \quad (\text{A.57})$$

where  $\epsilon_{ij}$  is the second rank strain tensor,  $X_{\alpha\beta}$  the second rank stress tensor,  $s_{ij\alpha\beta}^E$  the fourth rank compliance tensor,  $E_\nu$  the field vector, and  $d_{ij\nu}$  the third rank piezoelectric tensor. By employing the geometric rules for tensor

<sup>7</sup> This method of determining the constants for rotated axes is discussed in a former paper "Dynamic Measurements of the Constants of Rochelle Salt," *Phys. Rev.*, April 15, 1939, Appendix I.

<sup>8</sup> This method is discussed in a recent paper by W. L. Bond, "The Mathematics of The Physical Properties of Crystals," *B. S. T. J.*, Jan. 1943.

<sup>9</sup> The tensor method of writing the elastic and piezoelectric relations is discussed by Atanasoff and Hart and by Lawson. See references (2) and (3).



transformation of axes, the components of the rotated tensors are easily calculated and the elastic and piezoelectric constants for rotated crystals determined.

The variation of Young's modulus as a function of orientation was first worked out by Voigt. In terms of the *IRE* angles specifying the orientation of a crystal plate, the *s* compliance modulus (inverse of Young's Modulus) is given by the equation

$$s_{11}^{E'} = s_{11}^E (\cos^2 \theta \cos^2 \psi + \sin^2 \psi)^2 + (2s_{13} + s_{44}^E) \sin^2 \theta \cos^2 \psi \\ \times (\cos^2 \theta \cos^2 \psi + \sin^2 \psi) + s_{33} \sin^4 \theta \cos^4 \psi - 2s_{14}^E \sin \theta \sin \psi \cos \psi \quad (\text{A.58}) \\ \times [3(\cos \varphi \cos \theta \cos \psi - \sin \varphi \sin \psi)^2 - (\sin \varphi \cos \theta \cos \psi - \cos \varphi \sin \psi)^2]$$

As discussed in Chapter II by W. L. Bond,<sup>10</sup> the *IRE* angles are measured as follows: Taking the  $X'$  axis along the length of the crystal, the  $Y'$  along the width, and the  $Z'$  along the thickness, the angle  $\theta$  is the angle between the  $Z$  or optic axis and  $Z'$ .  $\varphi$  is the angle between the projection of the  $Z'$  axis on the  $XY$  plane and the  $X$  axis, while  $\psi$  the skew angle is the angle between the length and the tangent to the great circle which contains the  $Z$  and  $Z'$  axes and the length of the crystal  $X'$ . A crystal having its thickness along the  $X$  axis ( $X$ -cut crystal) will have the angles

$\theta = 90^\circ$ ;  $\varphi = 0^\circ$ ;  $\psi$  variable but equal to  $90^\circ$  when the length coincides with the  $Y$  axis. Under these conditions

$$s_{11}^{E'} = s_{11}^E \sin^4 \psi + (2s_{13} + s_{44}^E) \sin^2 \psi \cos^2 \psi \\ + s_{33} \cos^4 \psi - 2s_{14}^E \sin^3 \psi \cos \psi \quad (\text{A.59})$$

This equation has been made use of in evaluating the elastic constants of quartz as shown by equations (A.20). For this equation  $A_2$  was measured from the  $Y$  axis rather than from the  $Z$  as in the *IRE* angle and

$$A_2 = \psi - 90^\circ \quad (\text{A.60})$$

Since from equation (A.19) the frequency of a long thin crystal in longitudinal motion is known to be

$$f = \frac{1}{2\ell} \sqrt{\frac{1}{\rho s_{11}^{E'}}} \quad (\text{A.19})$$

the longitudinal frequency of any oriented crystal can be calculated from equations (A.58) and (A.19).

It is the purpose of this section to show also that the temperature coefficient of the longitudinal frequency of any oriented crystal can be calculated provided we know the temperature coefficient of the six elastic constants of

<sup>10</sup> Methods for Specifying Quartz Crystal Orientation and their Determination by Optical Means," this issue of the *B. S. T. J.*

quartz, and that regions of low temperature coefficient crystals can be located for this and other simple modes of motion for which the frequency can be calculated in terms of the elastic constants.

Differentiating equation (A.19) with respect to  $t$  the temperature

$$\frac{df}{dt} = -\frac{1}{2\ell} \sqrt{\frac{1}{\rho s_{11}^{E'}}} \left[ + \frac{d\ell}{dt} + \frac{1}{2} \left[ \frac{d\rho}{dt} + \frac{ds_{11}^{E'}}{s_{11}^{E'}} \right] \right] \text{ or} \tag{A.61}$$

$$\frac{\frac{df}{dt}}{f} = T_f = -T_\ell - \frac{1}{2} [T_\rho + T_{s_{11}^{E'}}]$$

where  $T_\alpha$  the temperature coefficient of the quantity  $\alpha$  is defined as the rate of change of  $\alpha$  with temperature divided by the value of  $\alpha$ . The temperature coefficient of the length  $\ell = X'$  is 7.8 parts per million per degree centigrade along the optic axis, and 14.3 parts per million perpendicular to it. For a general orientation, the temperature coefficient of length varies as

$$T_\ell = 14.3 - 6.5(\sin^2 \theta \cos^2 \psi) \tag{A.62}$$

Since the total mass remains the same when the crystal expands, the temperature coefficient of the density is the negative of the sum of the coefficients of the three axes or

$$T_\rho = -36.4 \tag{A.63}$$

Hence the temperature coefficient of frequency becomes

$$T_f = 3.9 + 6.5 \sin^2 \theta \cos^2 \psi - \frac{1}{2} \left( \frac{ds_{11}^{E'}}{s_{11}^{E'}} \right) \tag{A.64}$$

Differentiating equation (A.58) we have as the temperature coefficient of a general orientation

$$T_f = 3.9 + 6.5 \sin^2 \theta \cos^2 \psi$$

$$\frac{1}{2} \left[ \frac{s_{11}^{E'} T_{s_{11}^{E'}} (\cos^2 \theta \cos^2 \psi + \sin^2 \psi)^2 + (2s_{13} T_{s_{13}} + s_{44}^{E'} T_{s_{44}^{E'}}) \times \sin^2 \theta \cos^2 \psi (\cos^2 \theta \cos^2 \psi + \sin^2 \psi) + s_{33} T_{s_{33}} \times \sin^4 \theta \cos^4 \psi - 2s_{14}^{E'} T_{s_{14}^{E'}} \sin \theta \sin \psi \cos \psi \times [3(\cos \varphi \cos \theta \cos \psi - \sin \varphi \sin \psi)^2 - (\sin \varphi \cos \theta \cos \psi + \cos \varphi \sin \psi)^2]}{s_{11}^{E'} (\cos^2 \theta \cos^2 \psi + \sin^2 \psi)^2 + (2s_{13} + s_{44}^{E'}) \sin^2 \theta \cos^2 \psi \times (\cos^2 \theta \cos^2 \psi + \sin^2 \psi) + s_{33} \sin^4 \theta \cos^4 \psi - 2s_{14}^{E'} \sin \theta \sin \psi \cos \psi [3(\cos \varphi \cos \theta \cos \psi - \sin \varphi \sin \psi)^2 - (\sin \varphi \cos \theta \cos \psi + \cos \varphi \sin \psi)^2]} \right] \tag{A.65}$$

Hence since the elastic constants are definitely known, the temperature coefficient of any longitudinally vibrating crystal can be obtained when the separate temperature coefficients are evaluated.

The temperature coefficients appearing in equation (A.65) can all be evaluated from the temperature coefficient angle curves for  $X$  cut rotated crystals shown by Fig. 1.19. For an  $X$  cut crystal equation (A.65) reduces to

$$T_f = 3.9 + 6.5 \cos^2 \psi$$

$$- \frac{1}{2} \left[ \frac{s_{11}^E T_{s_{11}^E} \sin^4 \psi + (2s_{13} T_{s_{13}} + s_{44}^E T_{s_{44}^E}) \sin^2 \psi \cos^2 \psi + s_{33} T_{s_{33}} \cos^4 \psi - 2s_{14}^E T_{s_{14}^E} \sin^3 \psi \cos \psi}{s_{11}^E \sin^4 \psi + (2s_{13} + s_{44}^E) \sin^2 \psi \cos^2 \psi + s_{33} \cos^4 \psi - 2s_{14}^E \sin^3 \psi \cos \psi} \right] \quad (\text{A.66})$$

The value of  $T_{s_{11}^E}$  is obtained directly for  $A_2 = 0$  or  $\psi = 90^\circ$ , for  $T_f = -2$  and hence

$$T_{s_{11}^E} = 11.8 \quad (\text{A.67})$$

Taking three other angles and solving for the remaining constants we find

$$T_{s_{14}^E} s_{14}^E = -5310; \quad (2s_{13} T_{s_{13}} + s_{44}^E T_{s_{44}^E}) = 45,130; \quad (\text{A.68})$$

$$T_{s_{33}} s_{33} = 17,400.$$

Inserting the values found for the elastic constants, two temperature coefficients are determined, and one relation is given between the others,

$$T_{s_{14}^E} = +119; \quad T_{s_{33}} = 182; \quad T_{s_{44}^E} = .1112 T_{s_{13}^E} = 228.2 \quad (\text{A.69})$$

The values of (A.68) are sufficient to determine the temperature coefficient of long thin crystals cut at any angle, for inserting these values in (A.65) the temperature coefficient for any oriented crystal in longitudinal vibration is given by

$$T_f = 3.9 + 6.5 \sin^2 \theta \cos^2 \psi$$

$$- \left[ \frac{+755 (\cos^2 \theta \cos^2 \psi + \sin^2 \psi)^2 + 22,565 \sin^2 \theta \cos^2 \psi (\cos^2 \theta \cos^2 \psi + \sin^2 \psi) + 8700 \sin^4 \theta \cos^4 \psi + 5310 \sin \theta \sin \psi \cos \psi [3(\cos \varphi \cos \theta \cos \psi - \sin \varphi \sin \psi)^2 - (\sin \varphi \cos \theta \cos \psi + \cos \varphi \sin \psi)^2]}{127.9 (\cos^2 \theta \cos^2 \psi + \sin^2 \psi)^2 + 175.8 \sin^2 \theta \cos^2 \psi (\cos^2 \theta \cos^2 \psi + \sin^2 \psi) + 95.6 \sin^4 \theta \cos^4 \psi + 89.2 \sin \theta \sin \psi \cos \psi [3(\cos \varphi \cos \theta \cos \psi - \sin \varphi \sin \psi)^2 - (\sin \varphi \cos \theta \cos \psi + \cos \varphi \sin \psi)^2]} \right] \quad (\text{A.70})$$

The only regions of low temperature coefficients are the regions for which the two big middle terms are small which requires that  $\theta \rightarrow 0$ , or  $\psi \rightarrow 90^\circ$ .

The first region would be a  $Z$ -cut crystal with its length somewhere in the  $XY$  plane and would result in a temperature coefficient of two parts per million negative. Such a crystal is not of much interest since there is no piezoelectric constant for driving it. The other region  $\psi \rightarrow 90^\circ$  would also result in the length being near the  $XY$  crystallographic plane, but would allow the major surface to be made perpendicular to the  $X$  axis and hence would allow the crystal to be driven piezoelectrically. By allowing  $\psi$  to be slightly greater than  $90^\circ$ , the fourth term in the numerator can be made slightly negative and of a value greater than the two positive terms. This results in the  $+5^\circ X$ -cut crystal having nearly a zero coefficient and this angle is the most favorable one for a low coefficient longitudinal mode of motion. All other directions have a negative temperature coefficient.

The remaining temperature coefficients of the six elastic constants can be evaluated from Fig. 1.12, and equation (A.22). The frequency temperature coefficient can be expressed by the equation:

$$T_f = 3.9 + 6.5 \cos^2 \theta + \frac{1}{2} \left[ \frac{c_{66}^E T_{c_{66}^E} \sin^2 \theta + c_{44}^E T_{c_{44}^E} \cos^2 \theta + T_{c_{14}^E} c_{14}^E \sin 2\theta}{c_{66}^E \sin^2 \theta + c_{44}^E \cos^2 \theta + c_{14}^E \sin 2\theta} \right] \quad (\text{A.71})$$

since in terms of the  $IRE$  angles the series of crystals is given by  $\varphi = -90^\circ$ ;  $\theta = 90 - A_2$ ;  $\psi = 90^\circ$ . Taking the  $AT$ ,  $BT$ , and  $Y$ -cut, whose coefficients have accurately been determined, we have

TABLE VI

Crystal Cut	Value of $A_2$	Value of $\theta$	$T_f$	$T_{c_{66}^E}$	$c_{66}^{E'}$
$AT$	$+35.25^\circ$	$54.75^\circ$	0	-12.0	$29.39 \times 10^{10}$ dynes/cm <sup>2</sup>
$Y$	0	90	+86	164.2	40.50
$BT$	-49	139 or -41	0	-15.2	68.86

From these data and equation (A.71), the three temperature coefficients can be evaluated as

$$T_{c_{66}^E} = 164.2; \quad T_{c_{44}^E} = 165.7; \quad T_{c_{14}^E} = +90.2 \quad (\text{A.72})$$

To convert these into compliance temperature coefficients we have to make use of the relations of equations (A.8)

$$s_{66}^E = 2(s_{11}^E - s_{12}^E) = \frac{c_{44}^E}{c_{44}^E c_{66}^E - c_{14}^{E2}}; \quad s_{14}^E = \frac{-c_{14}^E}{2(c_{44}^E c_{66}^E - c_{14}^{E2});}$$

$$s_{44}^E = \frac{c_{66}^E}{c_{44}^E c_{66}^E - c_{14}^{E2}}.$$

Differentiating these with respect to  $l$ , we have

$$\begin{aligned}
 T_{s_{66}}^E &= T_{c_{44}}^E - \left[ \frac{C_{44}^E C_{66}^E}{C_{44}^E C_{66}^E - C_{14}^{E^2}} (T_{c_{44}}^E + T_{c_{66}}^E) \right] + \frac{2C_{14}^{E^2}}{C_{44}^E C_{66}^E - C_{14}^{E^2}} T_{c_{14}}^E \\
 &= \frac{S_{11}^E}{S_{11}^E - S_{12}^E} T_{s_{11}}^E - \frac{S_{12}^E}{S_{11}^E - S_{12}^E} T_{s_{12}}^E \\
 T_{s_{14}}^E &= T_{c_{14}}^E - \left[ \frac{C_{44}^E C_{66}^E}{C_{44}^E C_{66}^E - C_{14}^{E^2}} (T_{c_{44}}^E + T_{c_{66}}^E) \right] + \frac{2C_{14}^{E^2}}{C_{44}^E C_{66}^E - C_{14}^{E^2}} T_{c_{14}}^E \\
 T_{s_{44}}^E &= T_{c_{66}}^E - \left[ \frac{C_{44}^E C_{66}^E}{C_{44}^E C_{66}^E - C_{14}^{E^2}} (T_{c_{44}}^E + T_{c_{66}}^E) \right] + \frac{2C_{14}^{E^2}}{C_{44}^E C_{66}^E - C_{14}^{E^2}} T_{c_{14}}^E
 \end{aligned} \tag{A.73}$$

TABLE VII

Temperature Coefficient	Present Determination	Previous Determination	Bechmann
$T_{s_{11}}^E$	+11.8	+12	+11.5
$T_{s_{12}}^E$	-1352	-1265	-1125
$T_{s_{13}}^E$	-294.8	-238	-148
$T_{s_{14}}^E$	+120	+123	+113
$T_{s_{33}}^E$	+182	+213	+180
$T_{s_{44}}^E$	+195.4	+189	+175
$T_{s_{66}}^E$	-134.2	-133.5	-119

TABLE VIII

Temperature Coefficient	Present Determination	Previous Determination	Atanasoff & Hart	Bechmann	Koga
$T_{c_{11}}^E$	-46.5	-54	-49.7	-48	-61.1
$T_{c_{12}}^E$	-3300	-2350	-3000	-2115	-
$T_{c_{13}}^E$	-697	-687	-580	-530	-
$T_{c_{14}}^E$	+90.2	+96	+107	+82	+110
$T_{c_{33}}^E$	-204.5	-251	-213	-208	-
$T_{c_{44}}^E$	-165.7	-160	-169	-151	-199
$T_{c_{66}}^E$	+164.2	+161	+170.1	+144	+199

Inserting the numerical values for the elastic constants and the temperature coefficients we have

$$\begin{aligned}
 T_{s_{66}}^E &= .883T_{s_{11}}^E + .1071T_{s_{12}}^E = -134.5; & T_{s_{14}}^E &= 121.4; \\
 & & T_{s_{44}}^E &= 195.4
 \end{aligned} \tag{A.74}$$

The value of  $T_{s_{14}}^E$  provides a check on the accuracy of measurement since it has been measured in two ways. The agreement is within about 2 per cent which shows the probable accuracy of the measurement. Combining the coefficients of (A.69) with those given by equation (A.74), the complete temperature coefficients are given in Table VII together with previous determinations<sup>11,12</sup>. The present determination differs from a previous determination by the writer due to the use of the elastic constants found here rather than Voigt's constants.

The temperature coefficients of the  $c_{ij}^E$  elastic constants are easily obtained from the  $s_{ij}^E$  constants by employing the relations of equation (A.8). These result in the temperature coefficient values for the  $c$  constants given in Table VIII.

By using the elastic constant data, the temperature coefficient data, and the equations of transformation for rotated axes it is possible to calculate the frequency and temperature coefficient of any simple mode for any orientation. Examples are given for a face shear mode and a thickness shear mode in a previous paper "Low Temperature Coefficient Quartz Crystals."<sup>13</sup> This paper shows contour maps for low temperature coefficient crystals of these types.

<sup>11</sup> The first determination of the temperature coefficients of the writer was given in a paper "Electrical Wave Filters Employing Quartz Crystals As Elements," *B. S. T. J.*, July 1934, p. 446. A redetermination using better temperature coefficient data was given in a paper "Low Temperature Coefficient Quartz Crystals," *B. S. T. J.*, Jan. 1940. The present determination uses the same temperature coefficient data but slightly different elastic constants which results in slight changes in the temperature coefficients.

<sup>12</sup> A partial determination of the coefficients was made by Koga, Rep. Rad. Research, Japan 6, 1 (1934). Other complete determinations are R. Bechmann, *Hoch: tech. U. Elek. Akus.* 44,145 (1934) and Atanasoff and Hart, *Phys. Rev.*, Vol. 59, No. 1, Jan. 1, 1941, pp. 85, 96.

<sup>13</sup> *B. S. T. J.*, Vol. XIX, 74 (Jan. 1940).